RIKEN QUANTUM COMPUTING

RIKEN

Quantum Spintronics Design:
Quantum Sensing with NV Centers in Diamond

Eisuke Abe

RIKEN Center for Quantum Computing

2025.9.3

47th Computational Materials Design (CMD®) Workshop

Spintronics Design Course (Online)

Diamond envy

©GIA

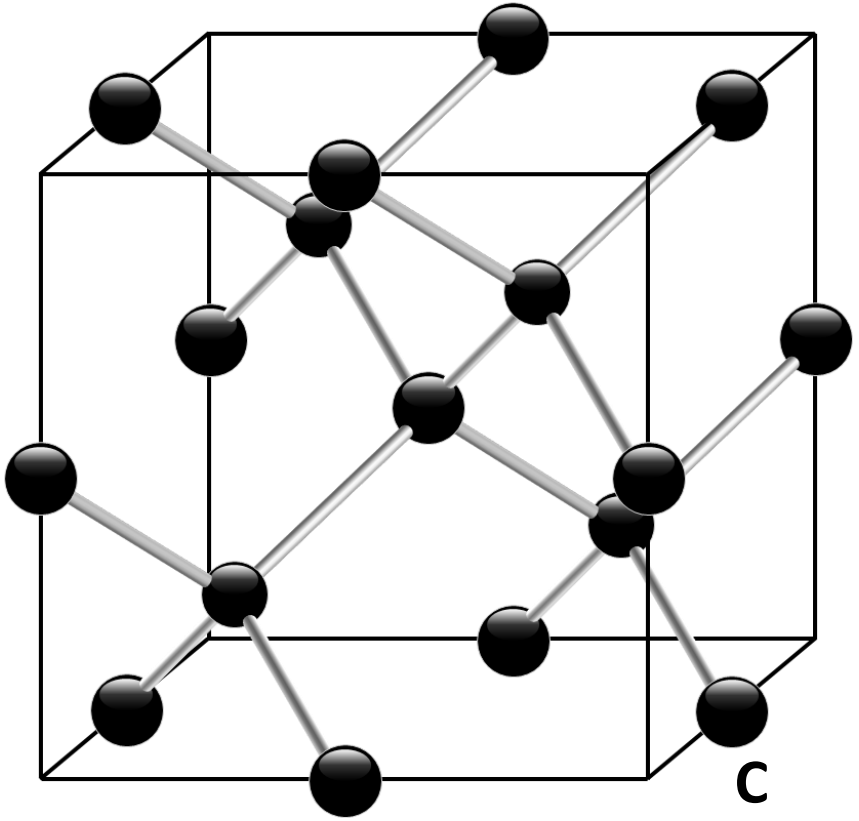

III (13)	IV (14)	V (15)
B	**C**	N

a = 0.357 nm

ρ = 1.77 x 10^{23} cm^{-3}

Diamond envy

©GIA

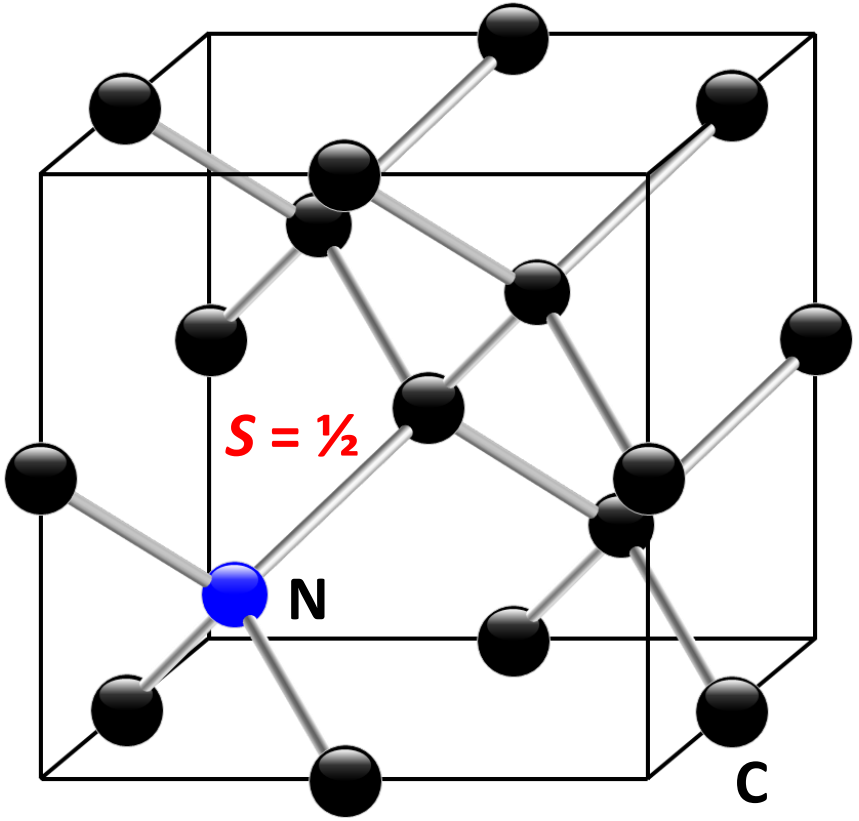

III (13)	IV (14)	V (15)
B	C	N

a = 0.357 nm

$\rho = 1.77 \times 10^{23}$ cm^{-3}

Types of diamond (% in natural diamonds)

- Ia: [N] < 3000 ppm, 98%
- Ib: [N] < 500 ppm, 0.1%
- IIa: [N] < 1 ppm, 1–2%
- IIb: [B] > 1 ppm, 0.1%

Diamond NV

©GIA

Our diamond: synthetic (CVD-grown)
2 x 2 x 0.5 mm^3, $700 (E6)
Type IIa, [N] < 5 ppb, [NV] < 0.03 ppb

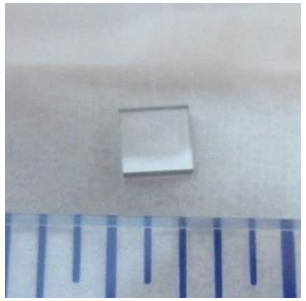

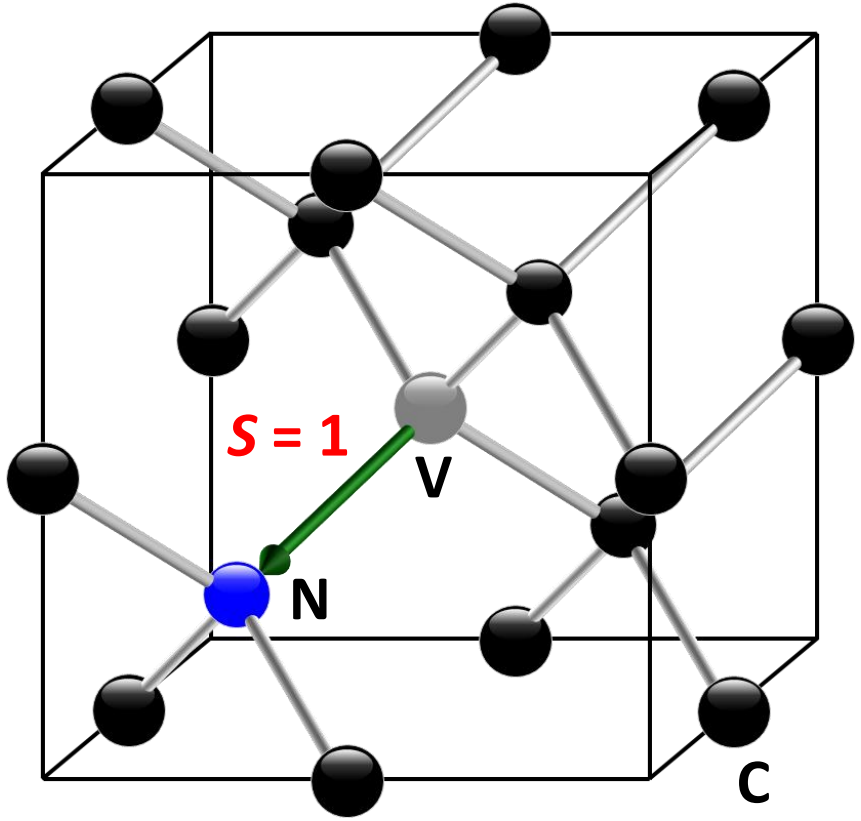

III (13)	IV (14)	V (15)
B	C	N

a = 0.357 nm
ρ = 1.77 x 10^{23} cm^{-3}

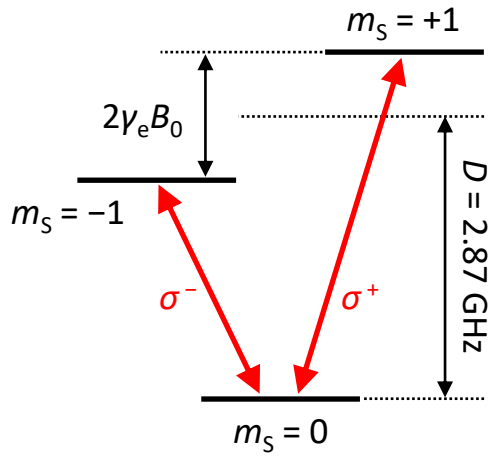

Quick overview of NV centers

- Optical detection & initialization of single spins
- Microwave control of single spins
- Room temperature operation

PL mapping

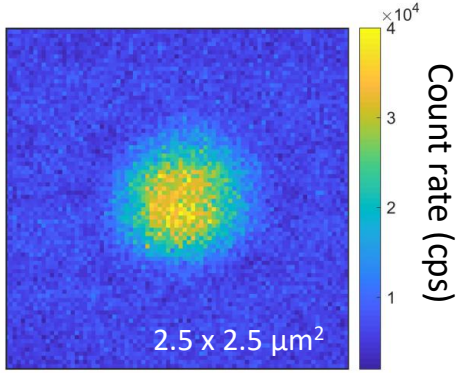

Optically detected magnetic resonance (ODMR)

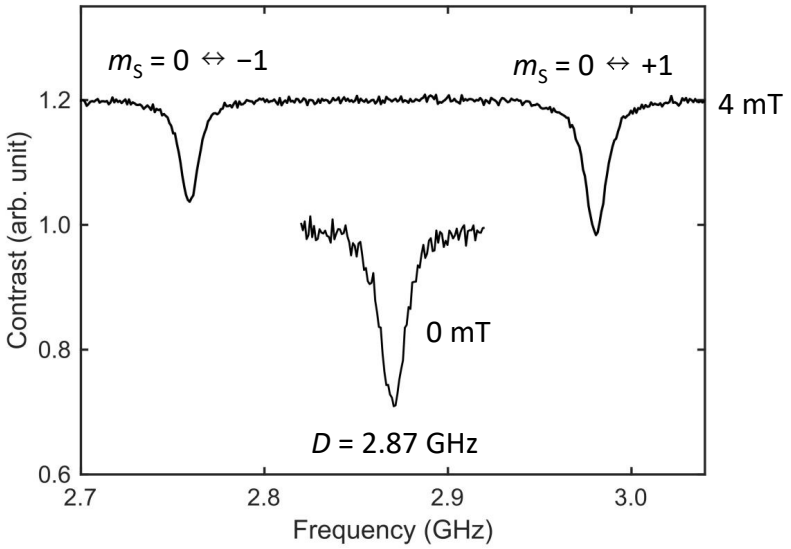

Rabi oscillation

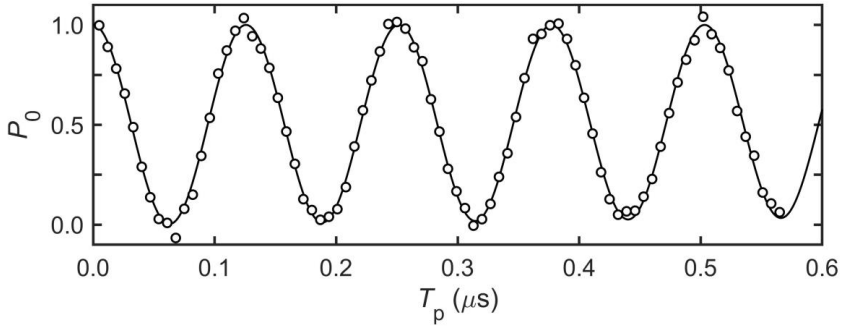

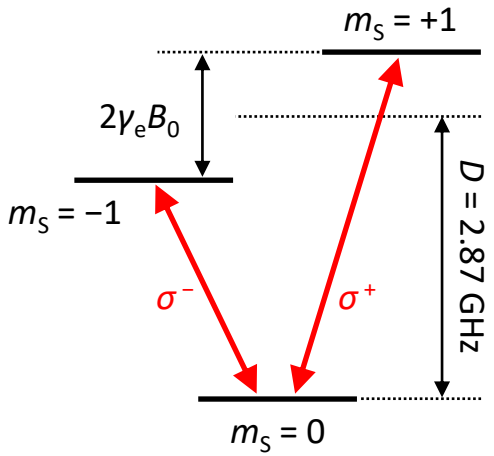

Quantum sensing with NV centers

- Sensitive to various physical quantities: *B*, *E*, *T*, *S*...
- Various modalities
- DC & AC modes
- High sensitivity
- High spatial resolution: μm–Å
- Wide temperature range: 800 K–mK
- Nondestructive

Nanodiamond & biology

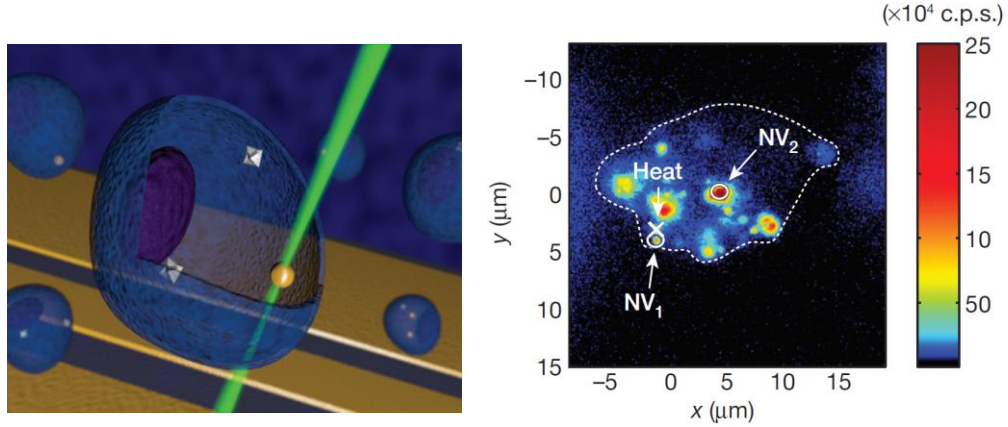

Nature **500**, 54 (2013)

Near-surface NV center & NMR

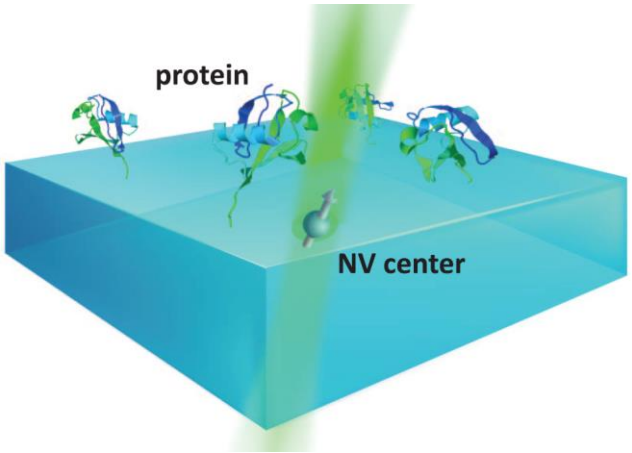

Science **351**, 836 (2016)

Scanning probe & condensed matter

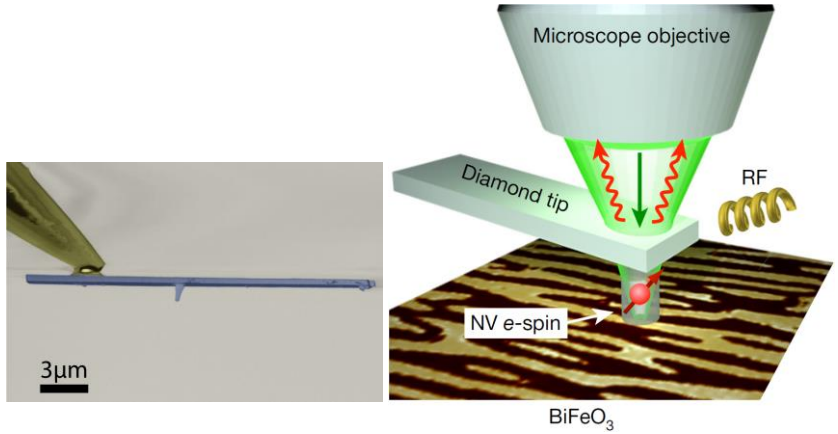

Rev. Sci. Instrum. **87**, 063703 (2016); Nature **549**, 252 (2017)

Wide-field imaging & geoscience/astrophysics

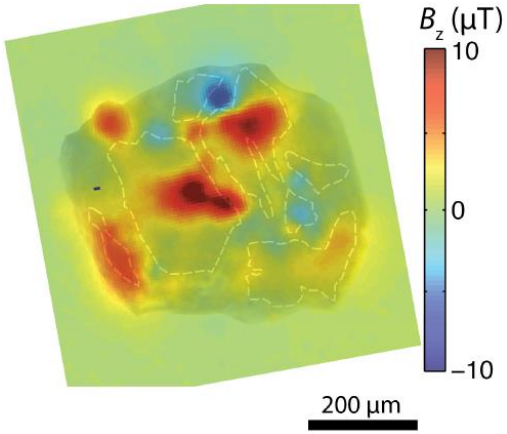

Science **346**, 1089 (2014)

Outline

- **Basics of NV centers in diamond**
  - Structure
  - Optical & magnetic properties

- **Basics of magnetic resonance**

- **Quantum sensing**
  - AC magnetometry
  - Detection of proton spin ensemble
  - Detection and control of a single proton spin

Outline

- **Basics of NV centers in diamond**
  - Structure
  - Optical & magnetic properties

- **Basics of magnetic resonance**

- **Quantum sensing**
  - AC magnetometry
  - Detection of proton spin ensemble
  - Detection and control of a single proton spin

Crystal & energy level structures

- Negatively-charged (NV^-)
- 4 sp^3 orbitals, 6 e^- (5 from the defect, 1 captured)
- C_{3v} (symmetry axis = quantization axis)
- 4 configurations in real space

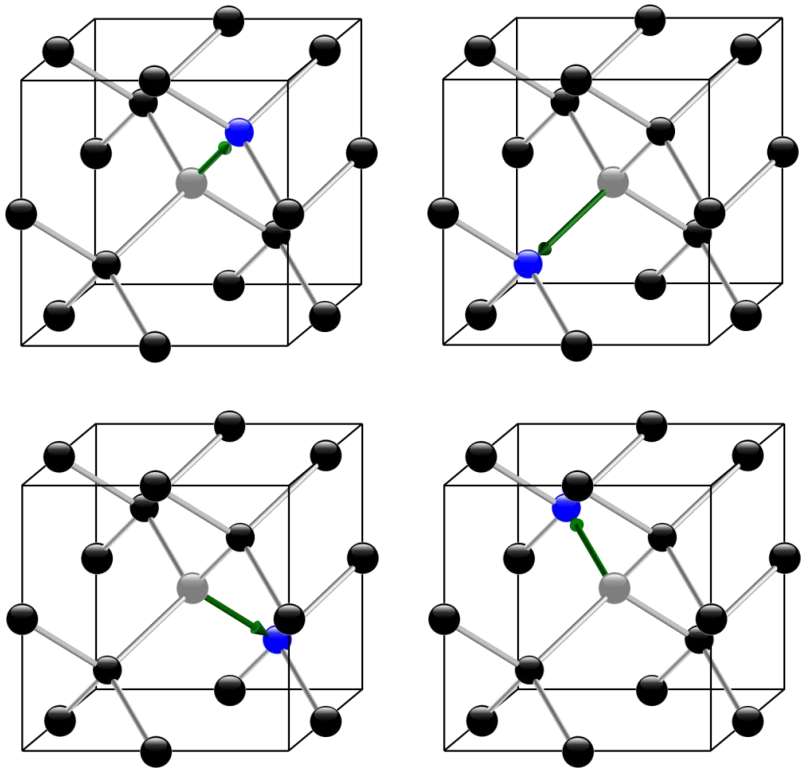

Effective spin-1 system (e^2-hole spin-triplet)

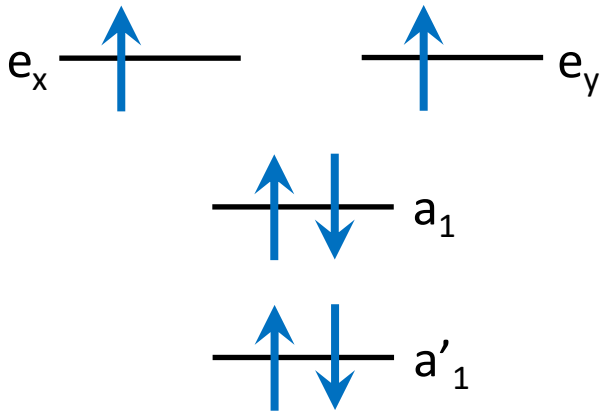

Energy levels

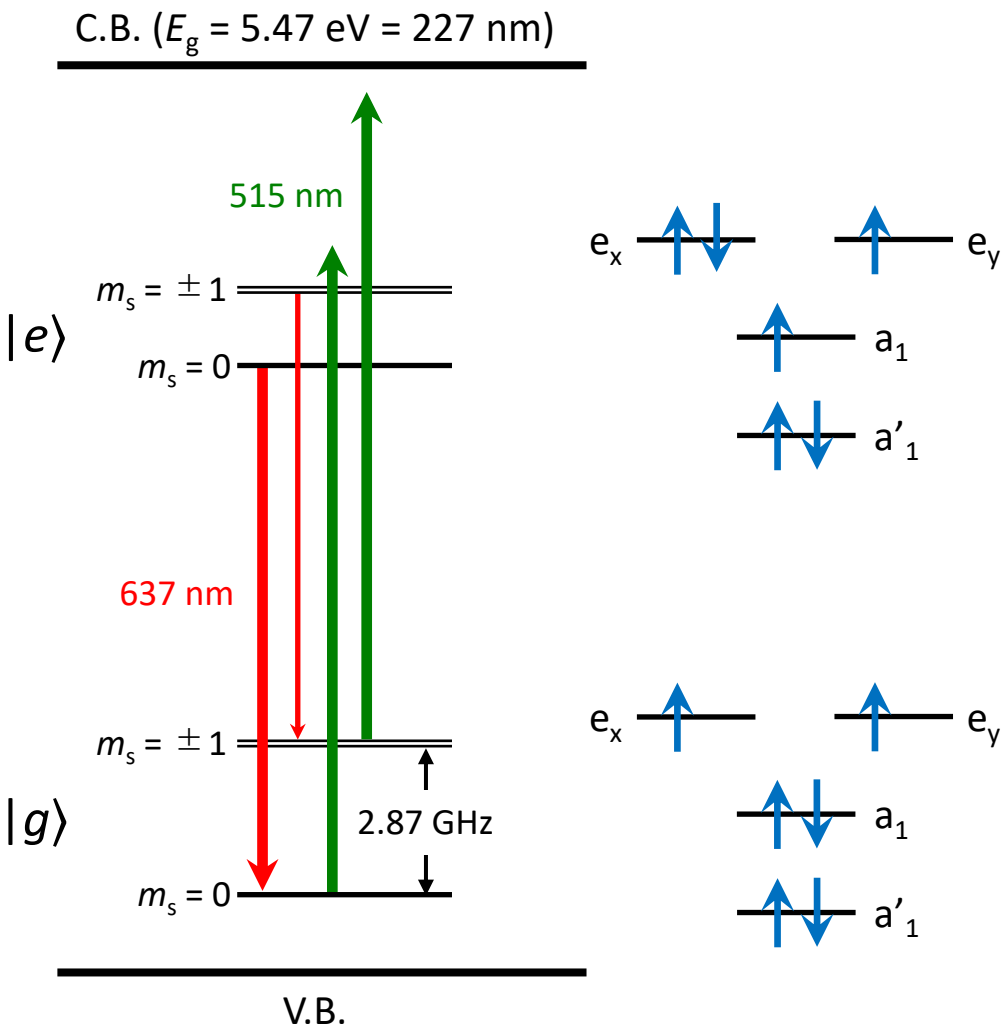

PL spectroscopy

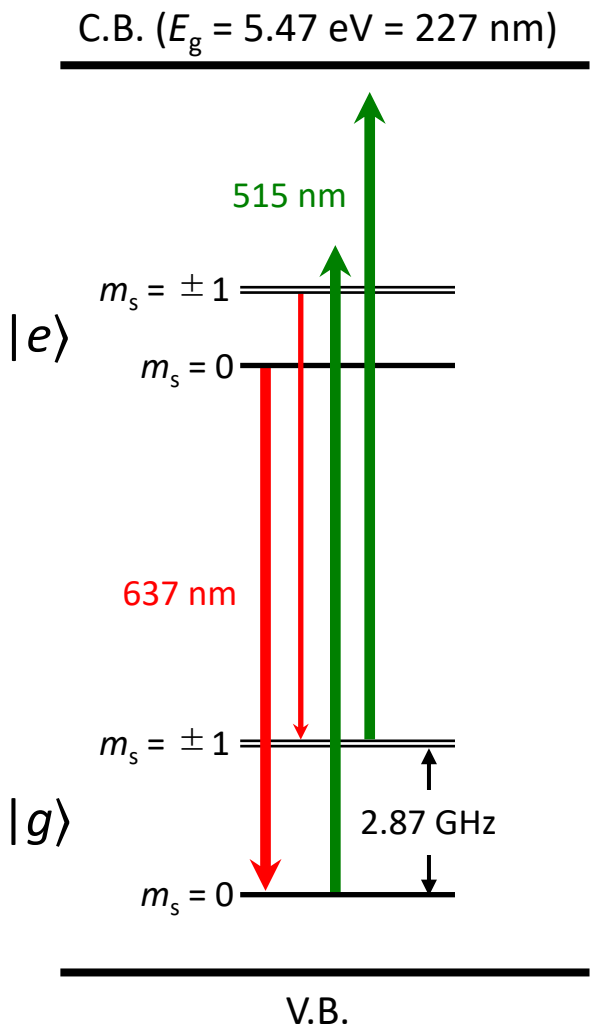

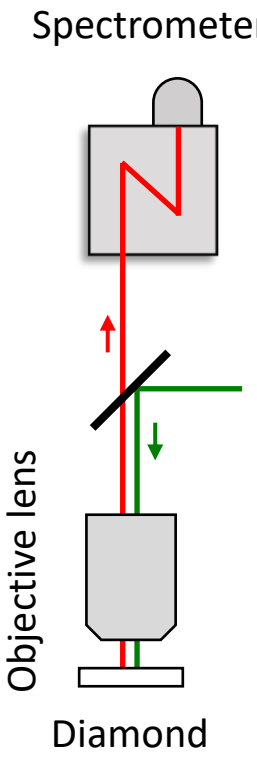

Zero-phonon line at 637 nm &
phonon-sideband up to 800 nm

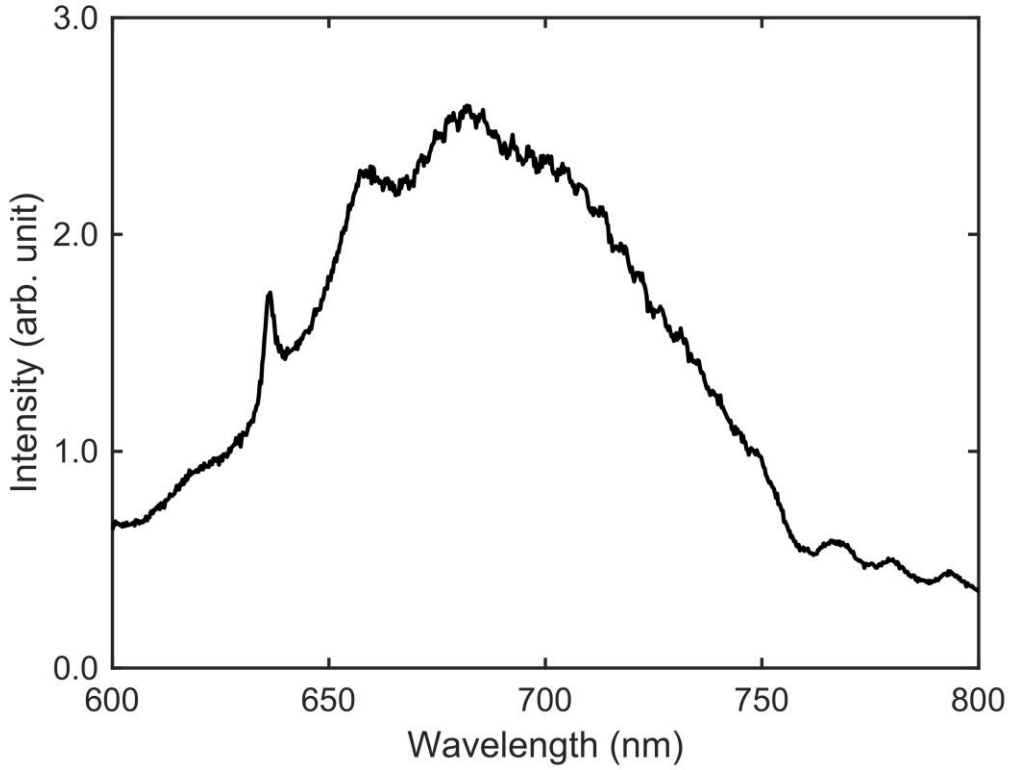

PL imaging

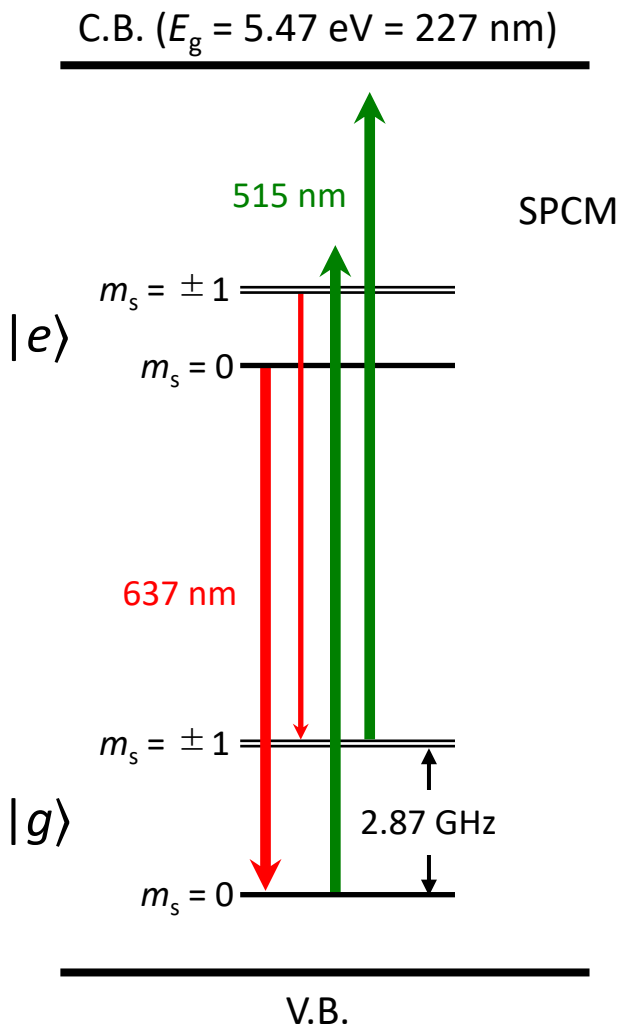

SPCM (single-photon counting module)
@600–800 nm

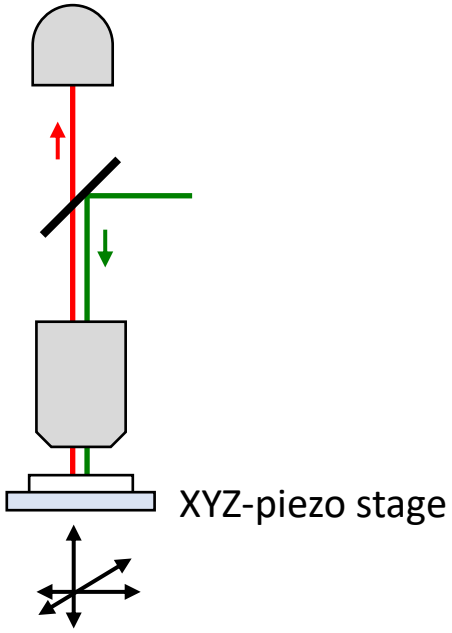

Optical diffraction limit = $\lambda_{exc}/(2NA)$

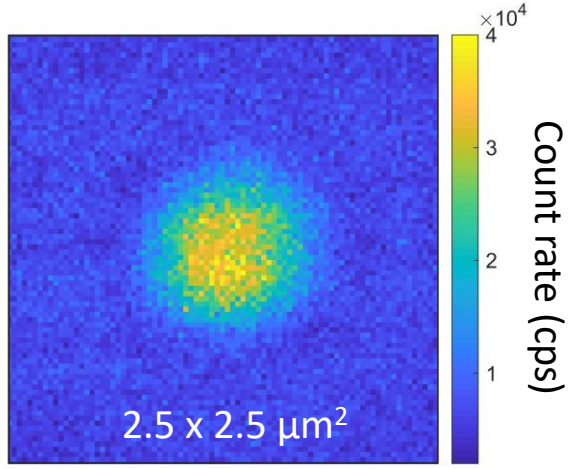

Photon statistics

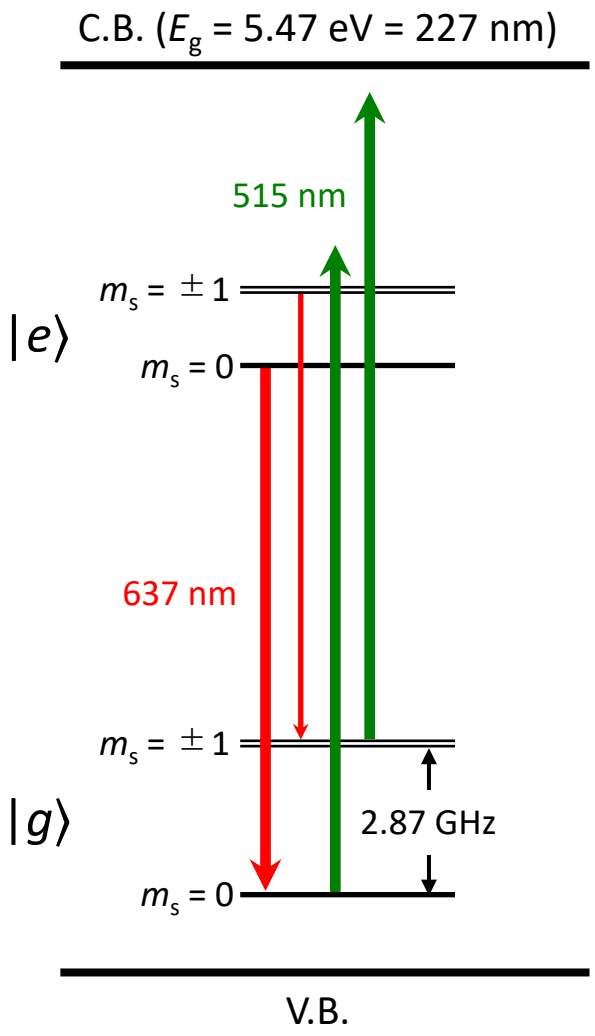

Timing analyzer

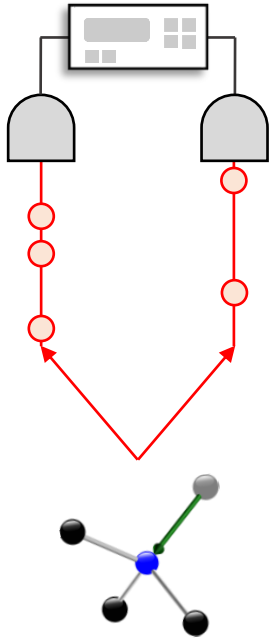

Single-photon source: one photon at a time

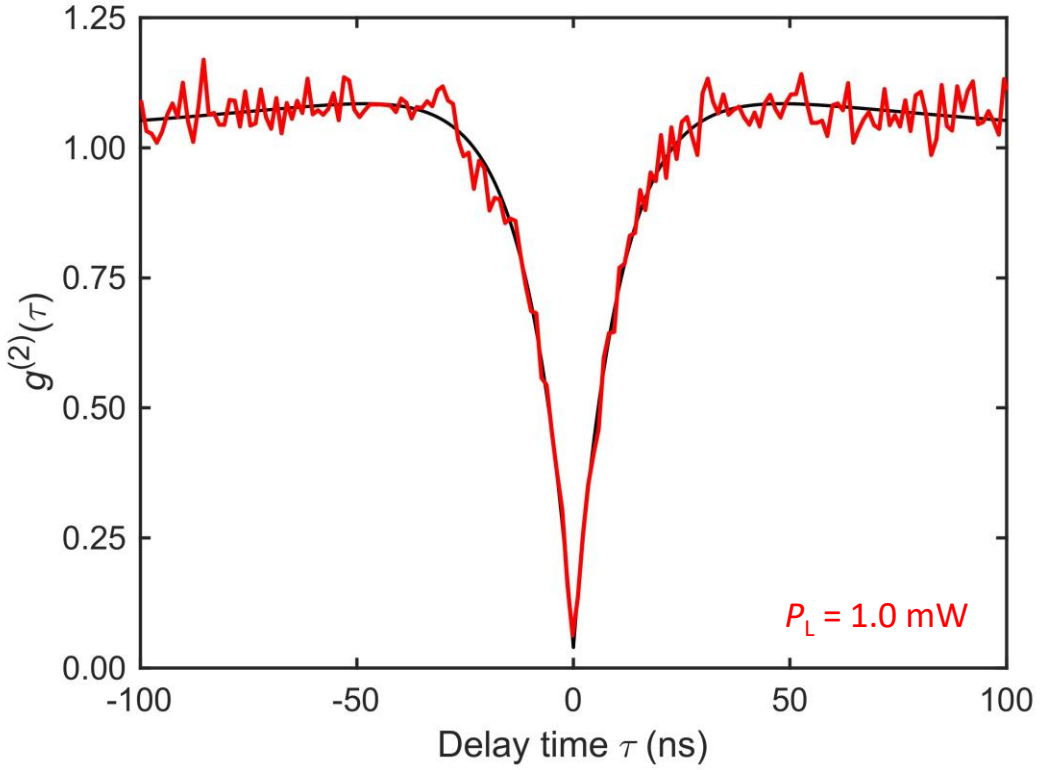

Time-resolved fluorescence

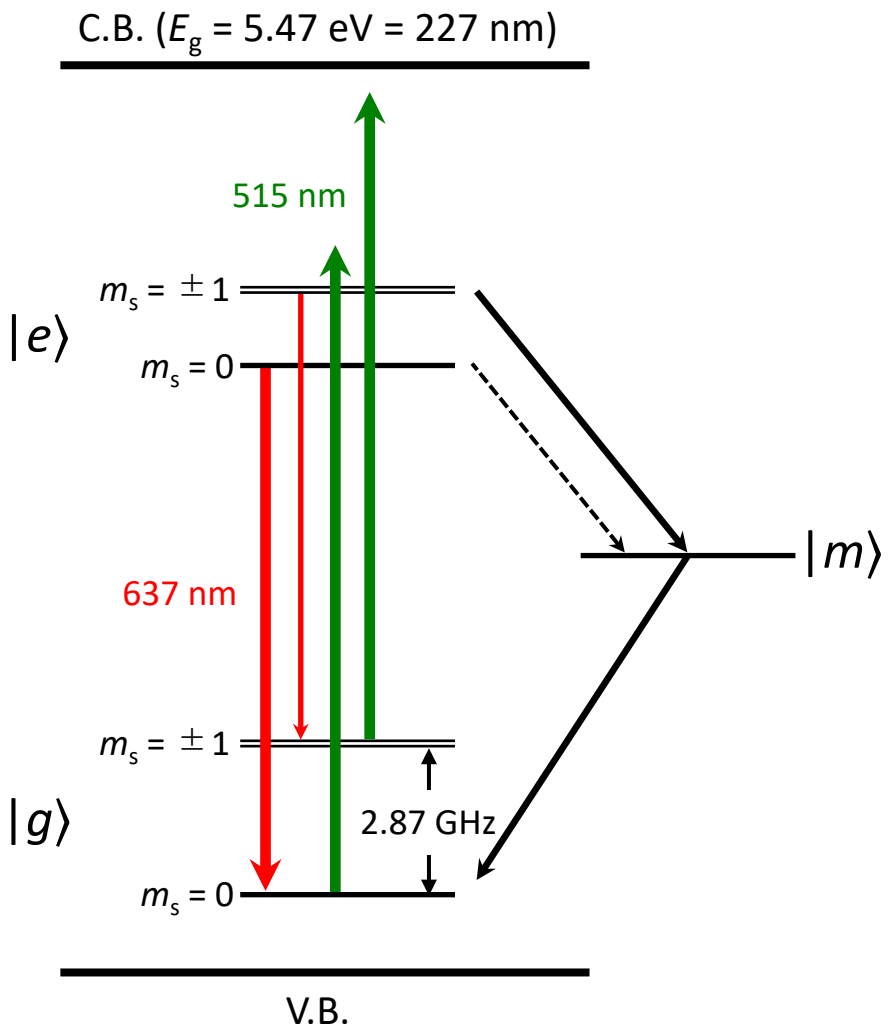

The **non-radiative** & **spin-selective** channel provides a means to **read out** & **initialize** the NV spin

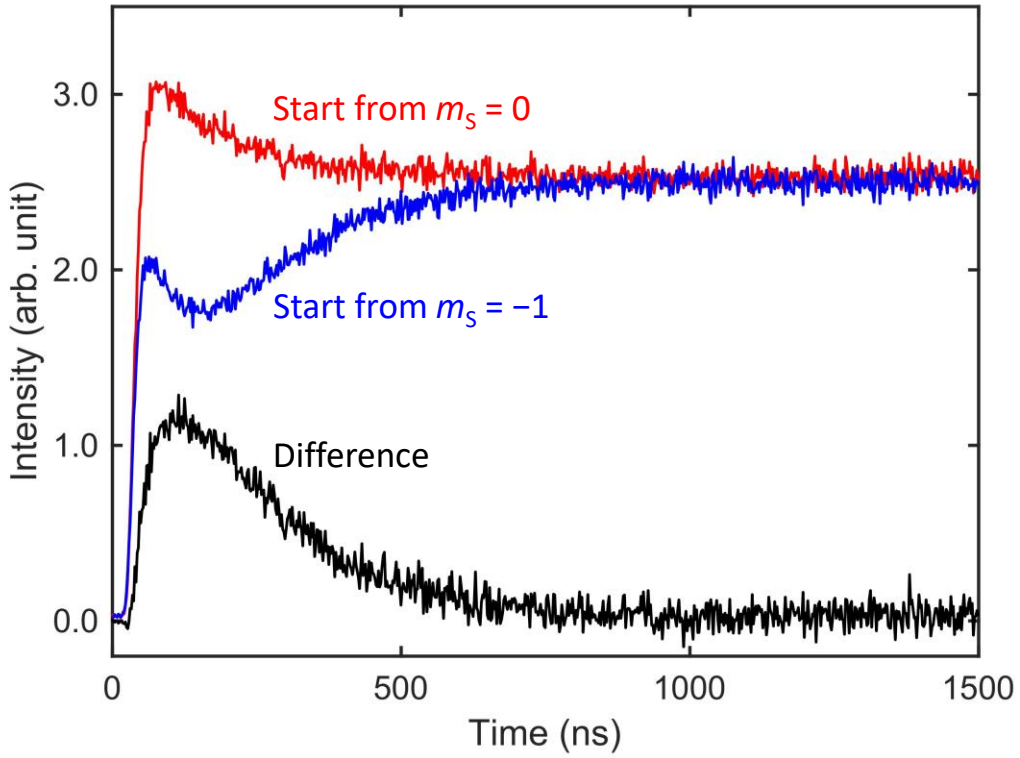

Optically detected magnetic resonance

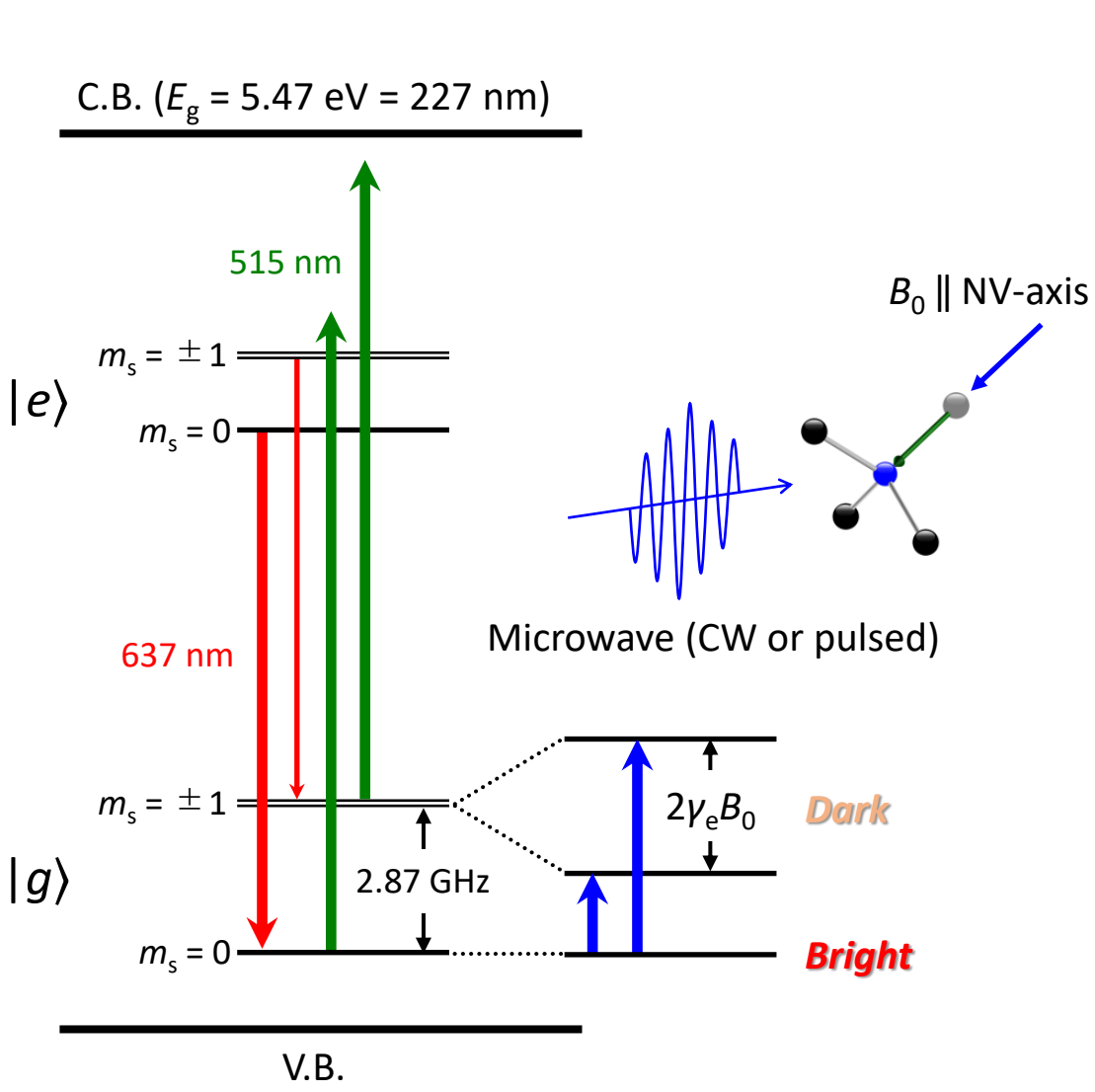

B_0 ∥ NV-axis

$$H = DS_z^2 + \gamma_e \boldsymbol{B}_0 \cdot \boldsymbol{S} = DS_z^2 + \gamma_e B_0 S_z$$

D = 2.87 GHz, γ_e = 28 MHz/mT

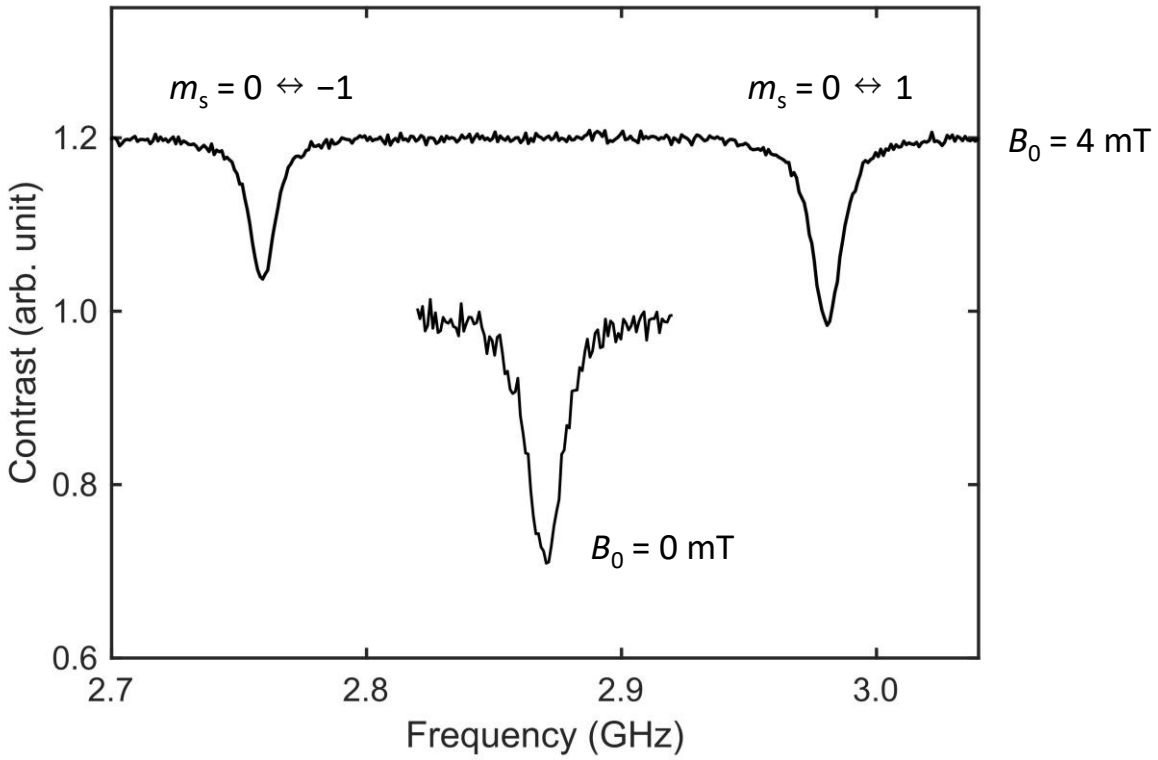

Experimental setup

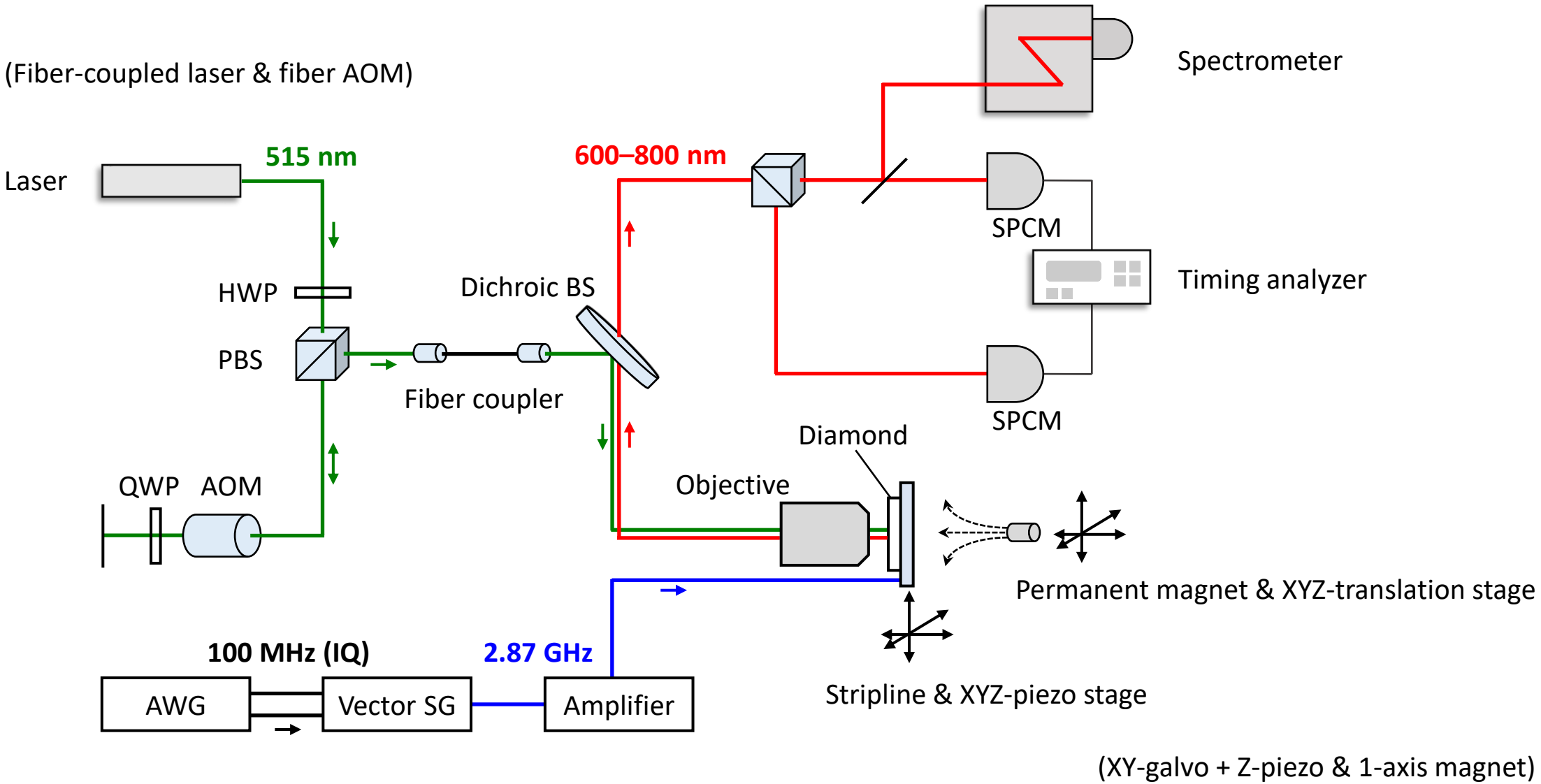

Experimental setup

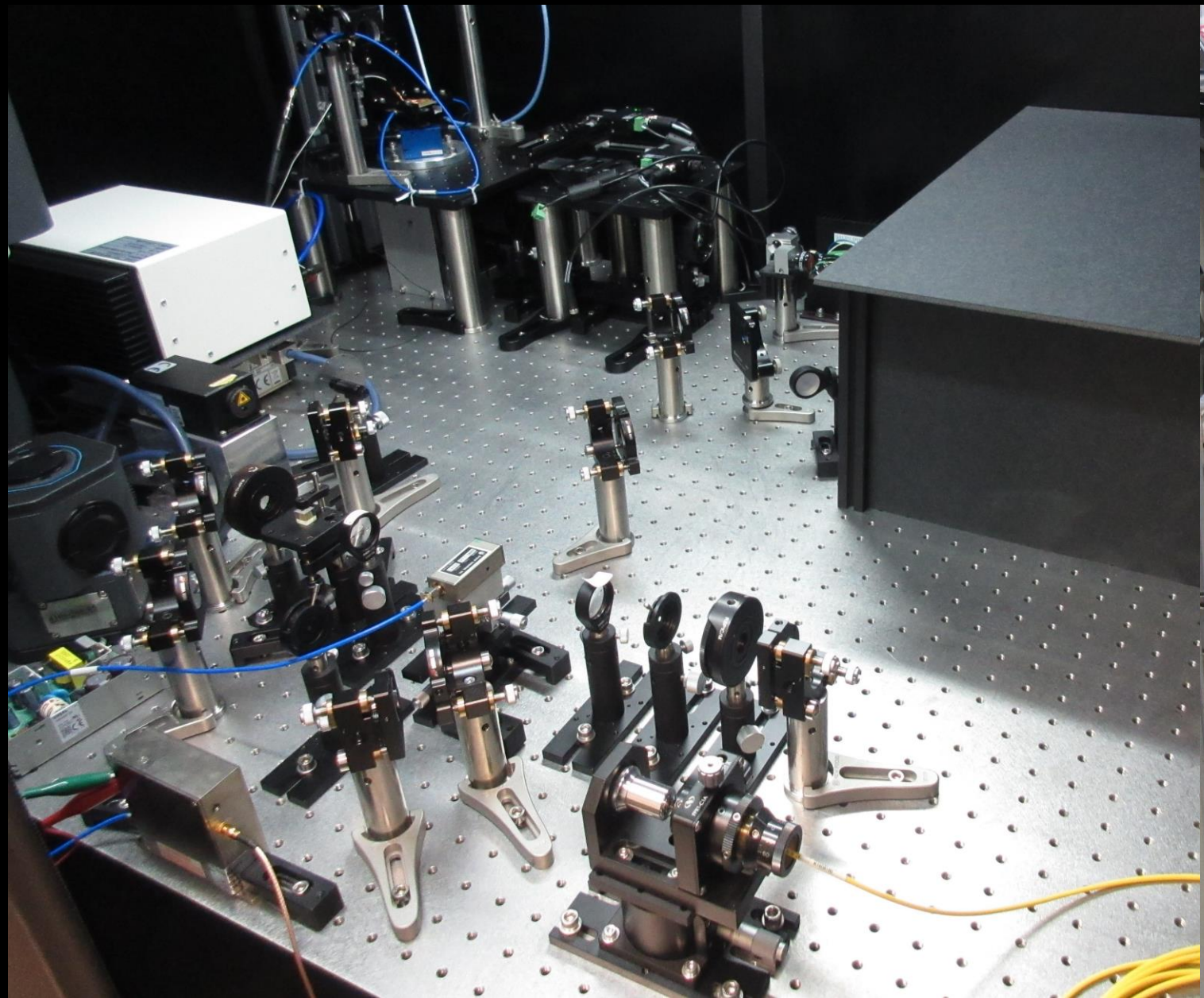

Experimental setup

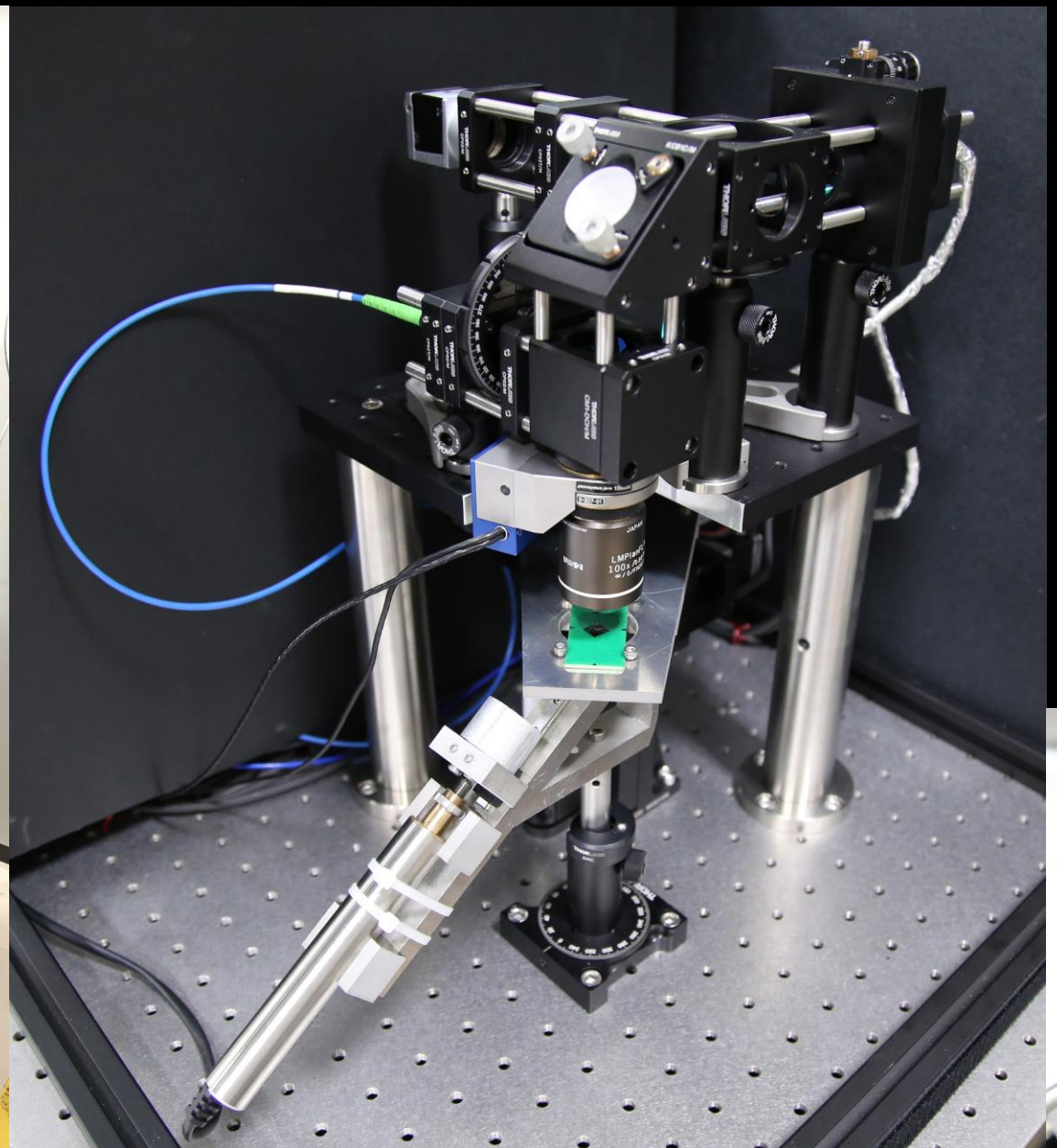

AIP Adv. **10**, 025206 (2020) Misonou *et al.*

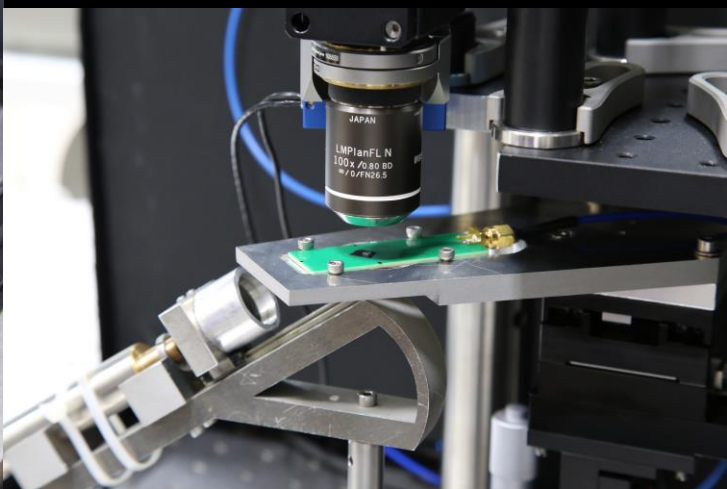

Outline

- **Basics of NV centers in diamond**
  - Structure
  - Optical & magnetic properties

- **Basics of magnetic resonance**

- **Quantum sensing**
  - AC magnetometry
  - Detection of proton spin ensemble
  - Detection and control of a single proton spin

Larmor precession

Torque equation

$$\frac{d\boldsymbol{\mu}}{dt} = \boldsymbol{\mu} \times \gamma \boldsymbol{B}_0$$

Gyromagnetic ratio ($g\mu_B$)

Magnetic moment: $\boldsymbol{\mu} = \gamma \boldsymbol{J}$

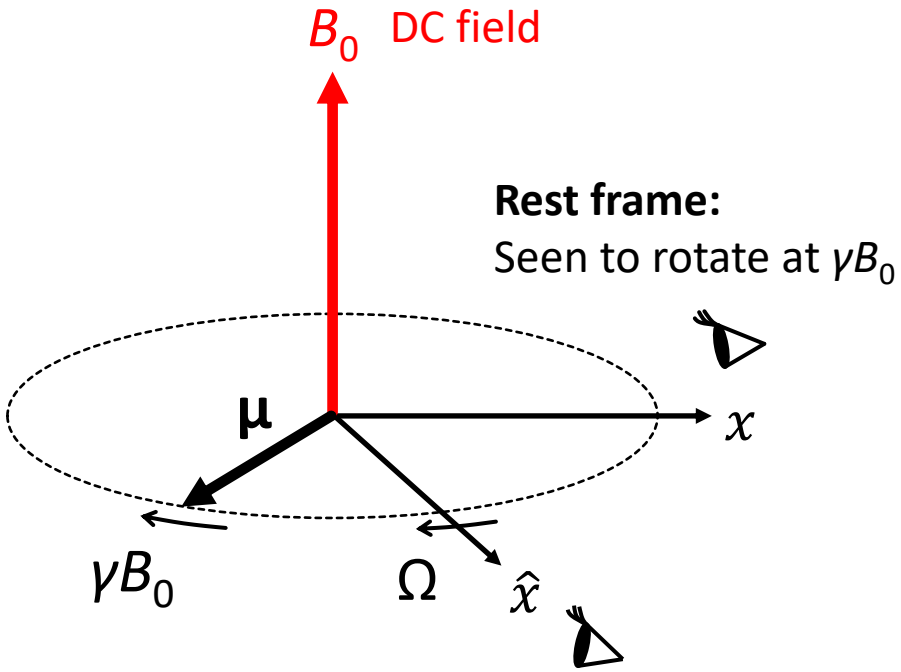

Frame rotating at angular velocity Ω:
Rotate slower…why?

Larmor precession

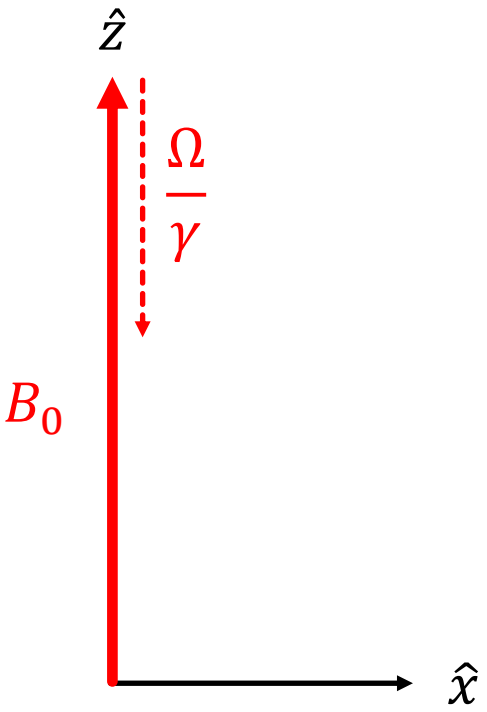

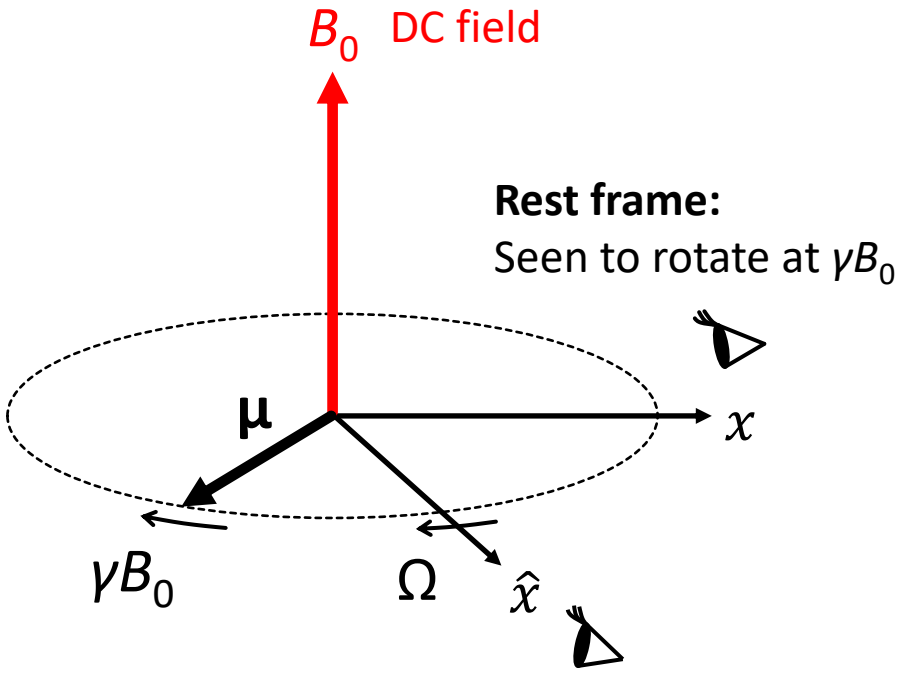

Frame rotating at angular velocity Ω:
Rotate slower…why?

DC field along the *z* direction becomes weaker

Magnetic resonance

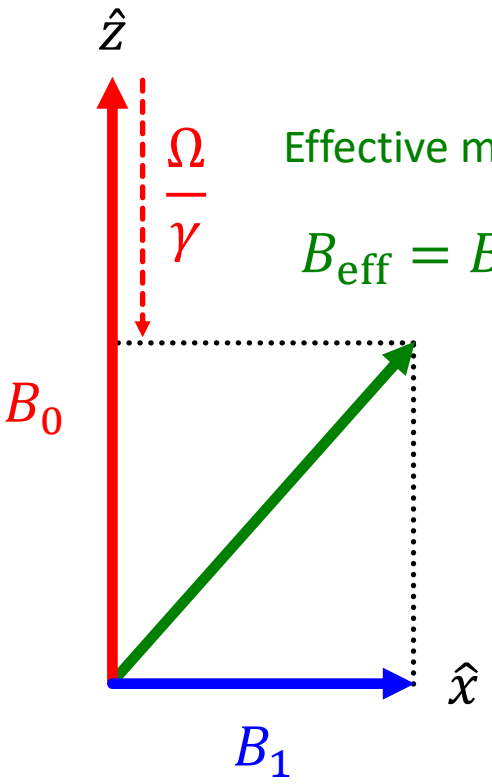

Effective magnetic field

$$B_{\text{eff}} = B_1\hat{x} + \left(B_0 - \frac{\Omega}{\gamma}\right)\hat{z}$$

AC field rotating in the *xy* plane at Ω

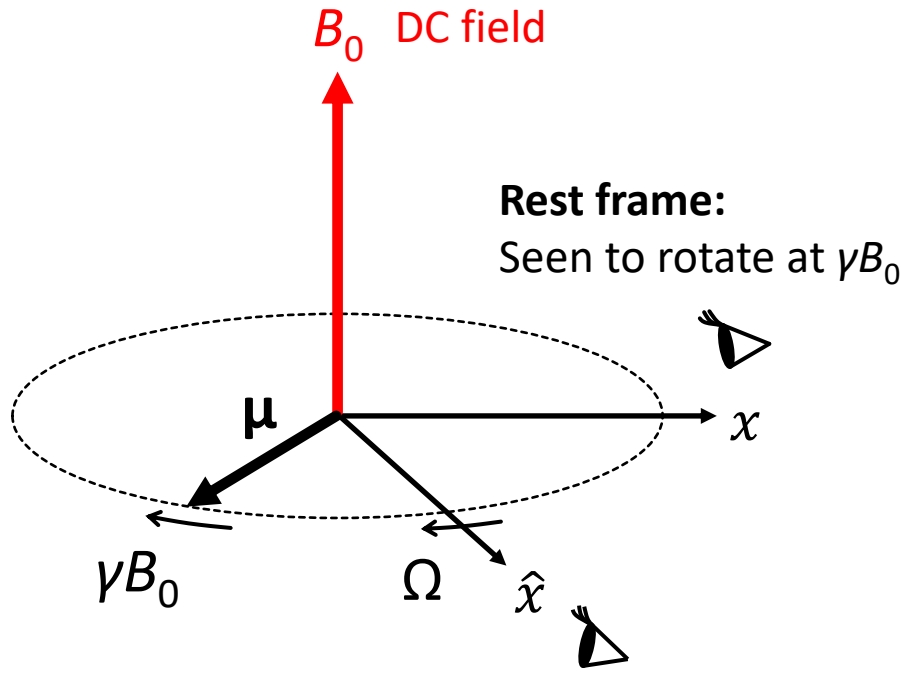

Frame rotating at angular velocity Ω:
Rotate slower…why?

DC field along the *z* direction becomes weaker

Magnetic resonance

Frame rotating at Ω = γB_0

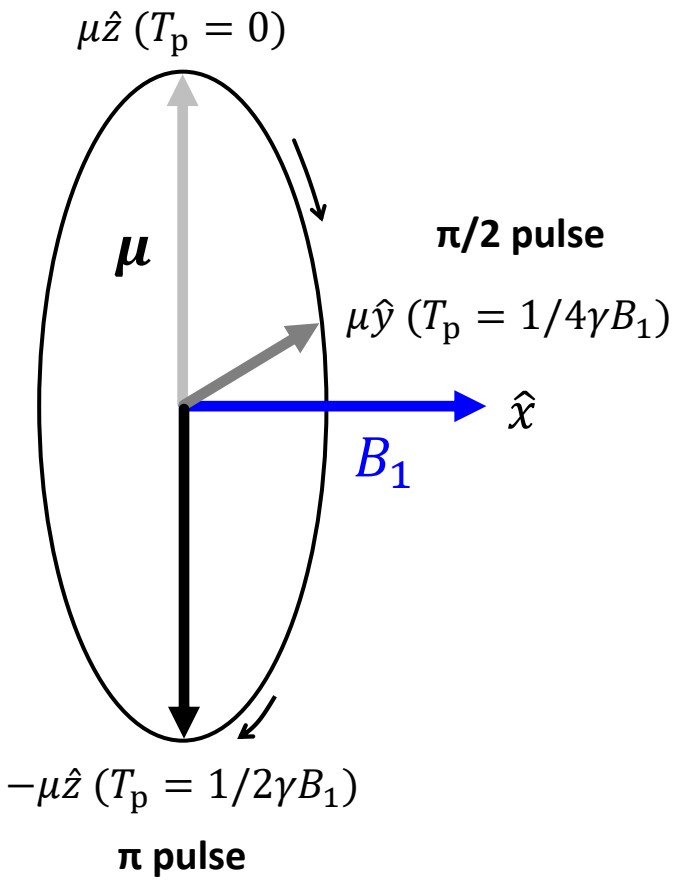

T_p: duration of B_1 field

Rest (non-resonant) frame

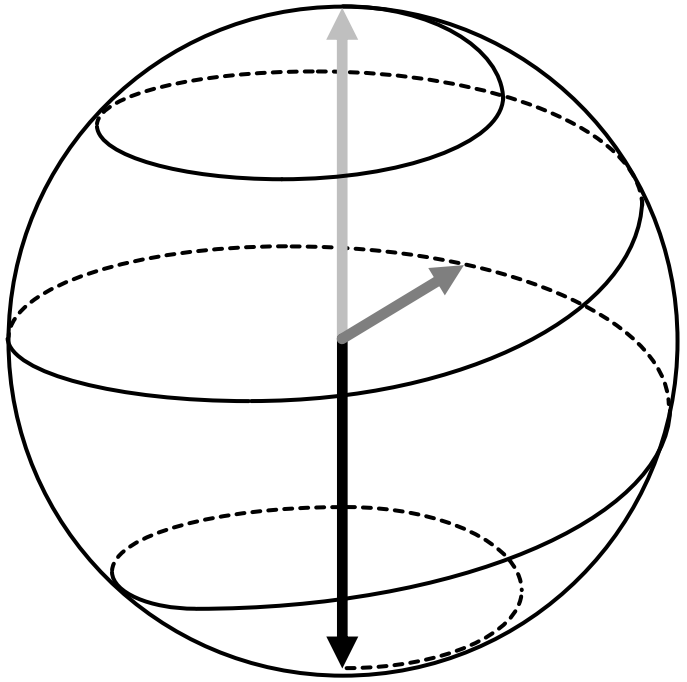

- Rotations about the $\pm\hat{x}, \pm\hat{y}$ axes are realized by adjusting the microwave phases
- Rotation about the $\hat{z}$ axis is superposed when observed from the rest (non-resonant) frame

Qubit & Bloch sphere

Qubit, spin-½ (NV is spin-1!)

$$\begin{cases} |"0"\rangle \equiv |m_s = 0\rangle \\ |"1"\rangle \equiv |m_s = -1\rangle \end{cases}$$

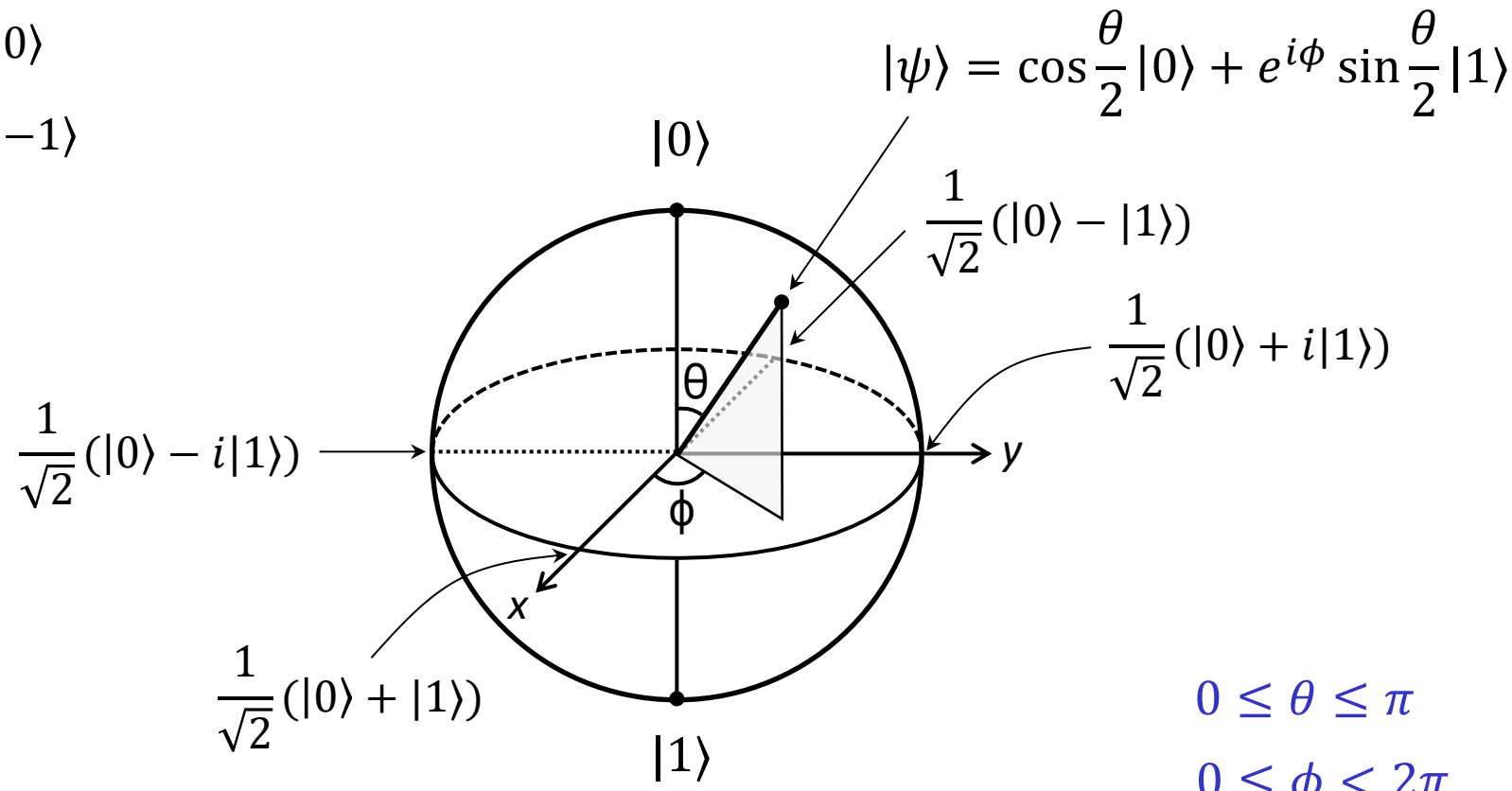

$0 \le \theta \le \pi$

$0 \le \phi < 2\pi$

Rabi oscillation

MW frequency fixed to one of the resonances
($m_s = 0 \leftrightarrow -1$ @$B_0 = 4.7$ mT)

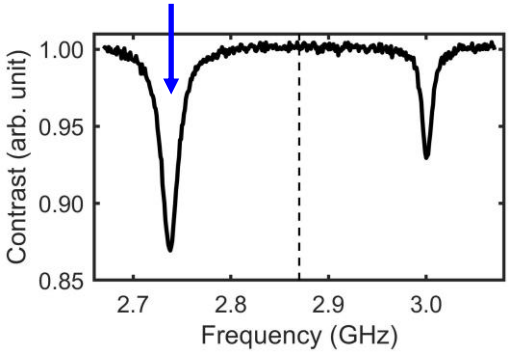

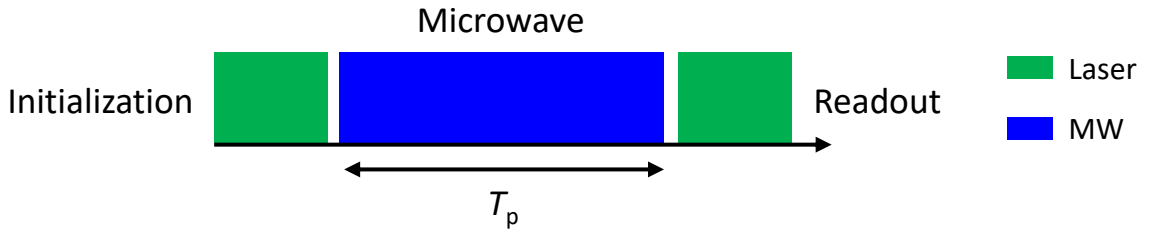

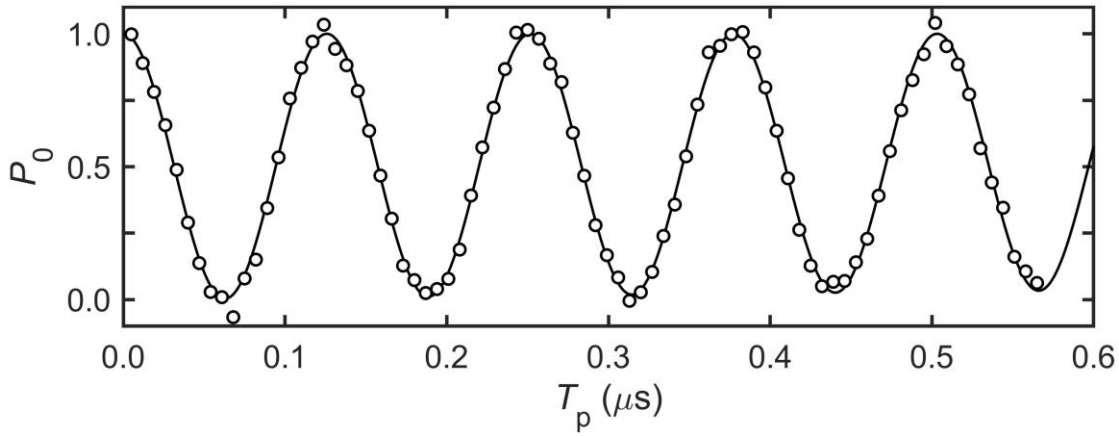

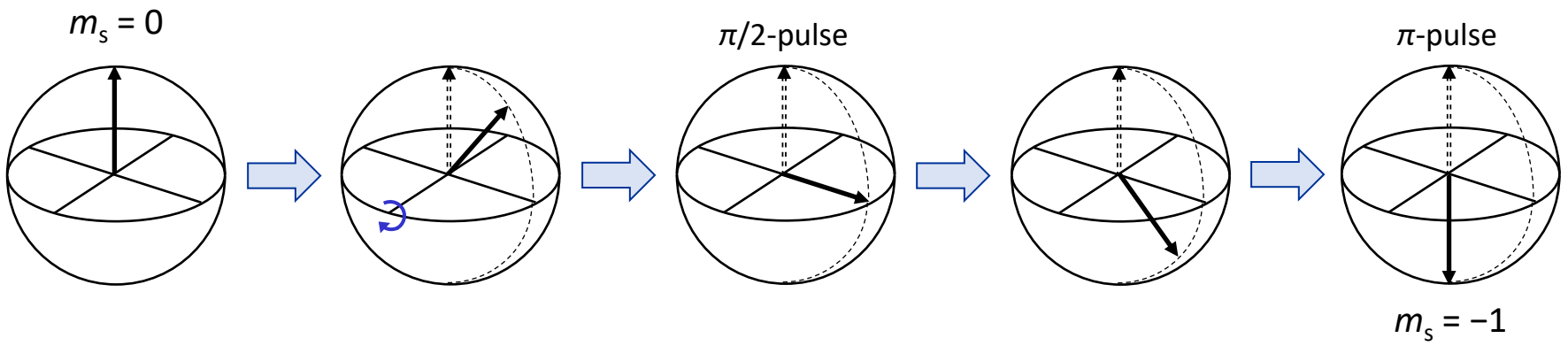

Quantum coherence

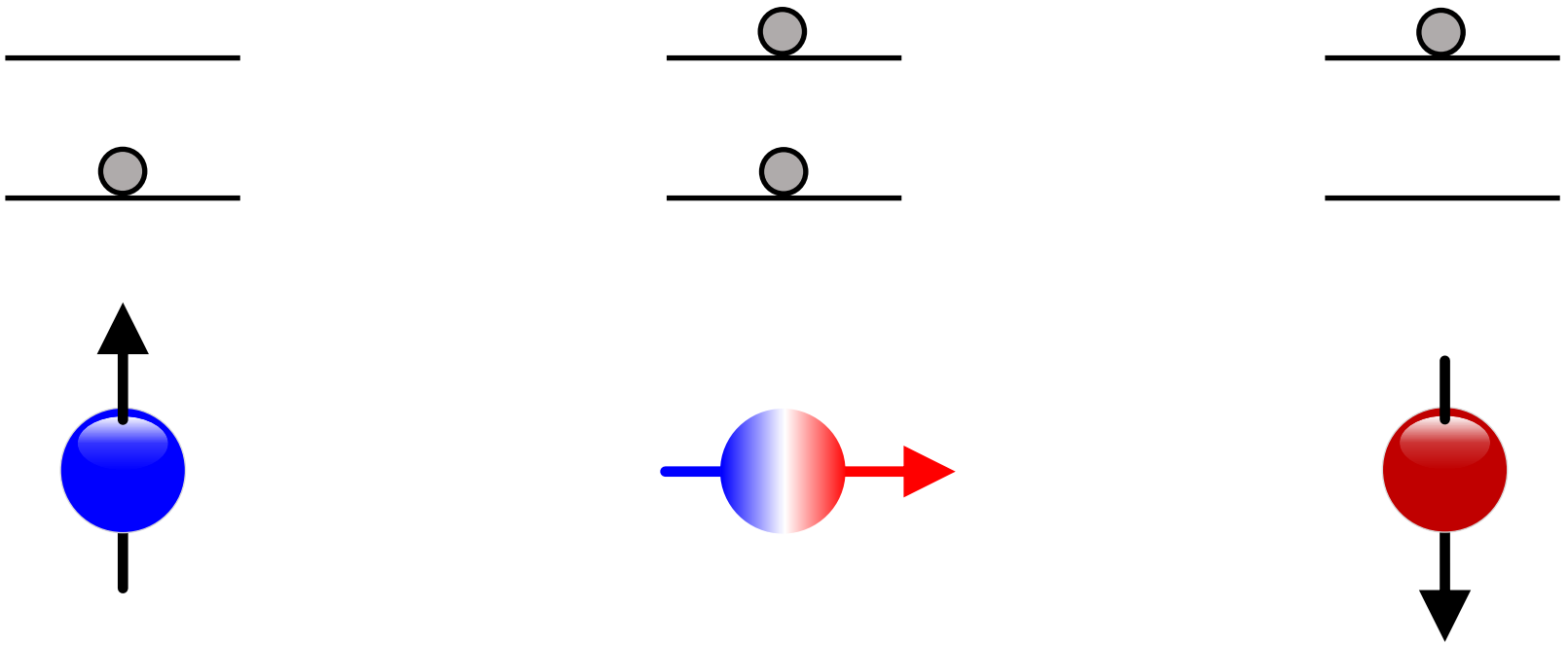

$|0\rangle \equiv |m_s = 0\rangle$ $\quad$ $|\Psi\rangle = \alpha|0\rangle + \beta|1\rangle$ $\quad$ $|1\rangle \equiv |m_s = -1\rangle$

T_2: measure of how long a superposition state is preserved

Relaxation times: T_1 & T_2

Bloch equation (Phenomenological description of incoherent spin dynamics)

$$\frac{d\boldsymbol{\mu}}{dt} = \boldsymbol{\mu} \times \gamma \boldsymbol{B}_0 - \frac{\boldsymbol{\mu}_{\parallel} - \boldsymbol{\mu}_0}{T_1} - \frac{\boldsymbol{\mu}_{\perp}}{T_2}$$

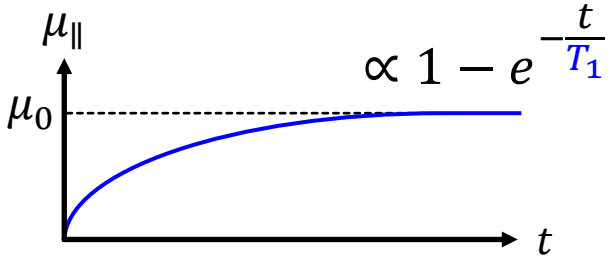

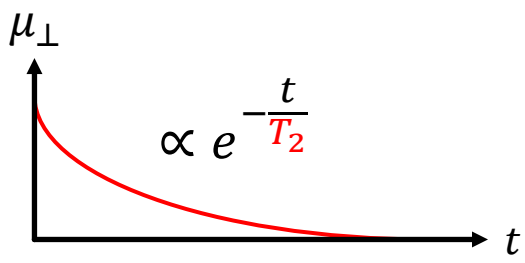

In typical spin systems, $T_1 >> T_2$

Energy relaxation (Change of the direction of a spin)

$$\frac{1}{T_1} = \frac{\gamma^2}{2} \int_{-\infty}^{\infty} \left[\langle b_x(\tau) b_x(0) \rangle + \langle b_y(\tau) b_y(0) \rangle \right] \cos(\omega_0 \tau)\, d\tau$$

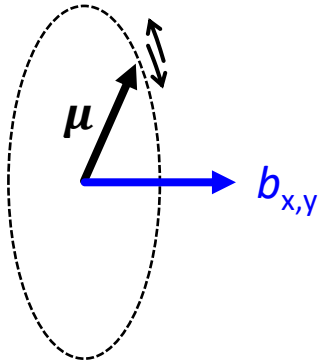

Phase relaxation (Random change of the precession frequency)

$$\frac{1}{T_2} = \frac{1}{2T_1} + \frac{\gamma^2}{2} \int_{-\infty}^{\infty} \langle b_z(\tau) b_z(0) \rangle d\tau$$

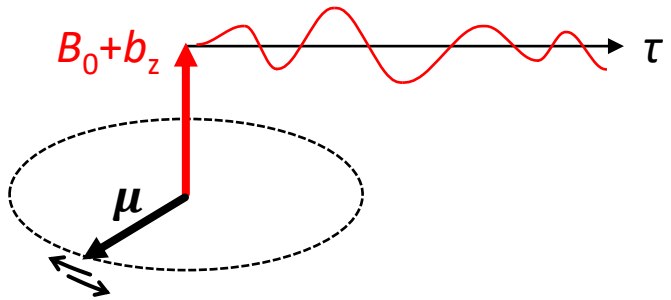

Measurement of T_2

Time domain → Decay of the transverse signal

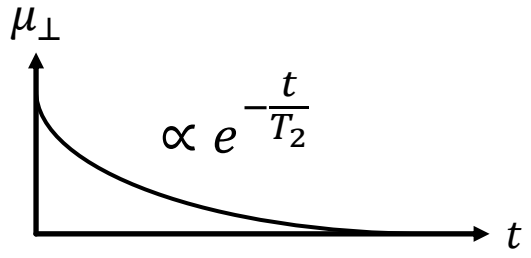

Frequency domain → Lorentzian

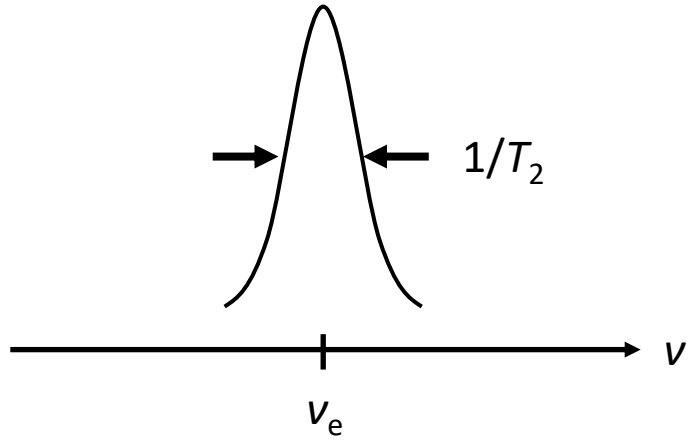

Stay along the *y* axis in the frame rotating at ν_e

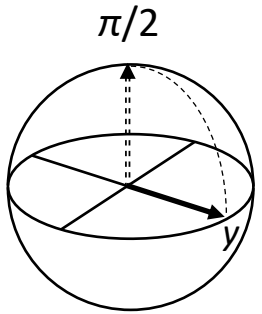

Measurement of T_2

Time domain → Decay of the transverse signal

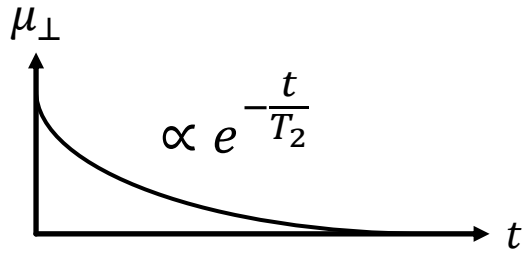

Frequency domain → Lorentzian

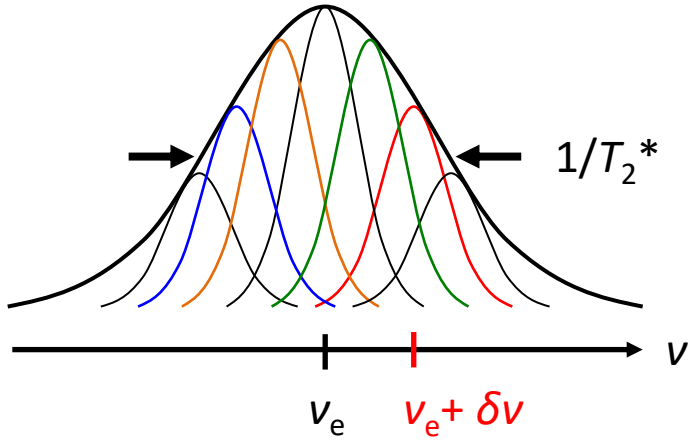

Precess at $\delta\nu$ in the frame rotating at ν_e

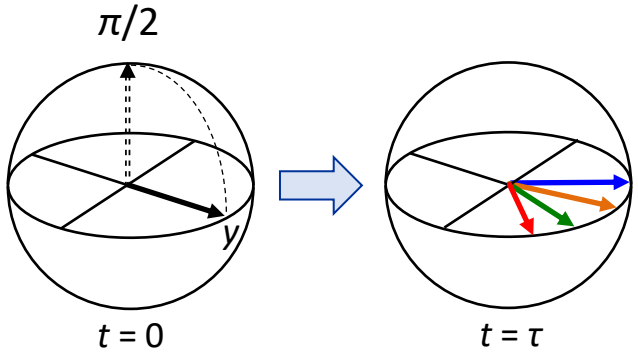

- Slow (> T_2) fluctuation of B_0 arising from magnet, nuclear spins…
- $\delta\nu$ is constant during a given run but varies in different runs (quasi-static)
- Many measurement runs
- Inhomogeneous line broadening

Spin echo

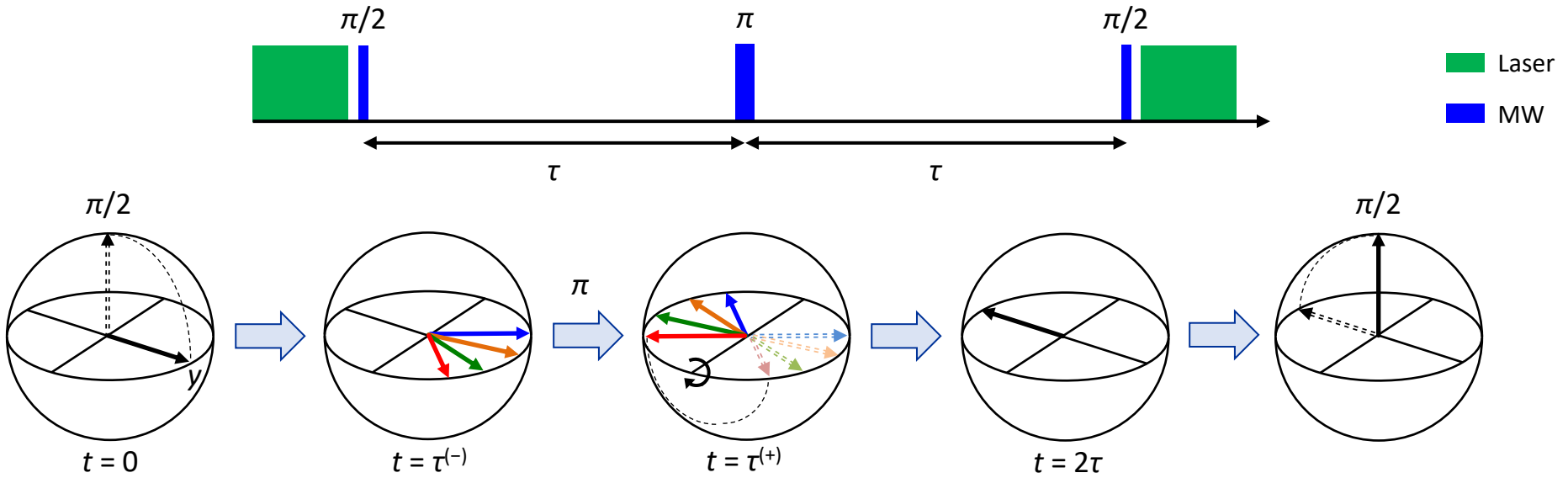

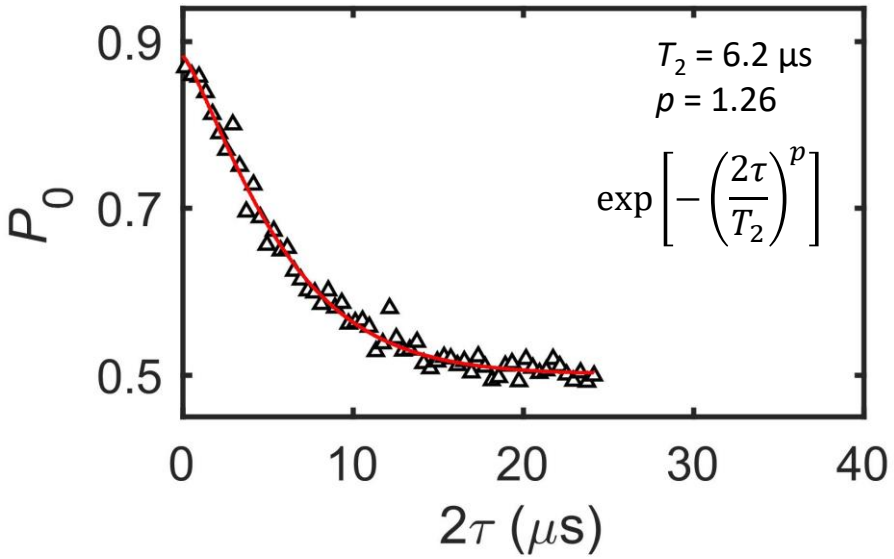

Static DC shifts are cancelled (refocusing)

Near-surface NV center

- N^+ implantation into ^{12}C (I = 0) layer
- d_{NV} = 6.26 nm
- B_0 = 23.5 mT

AIP Adv. **10**, 025206 (2020) Misonou *et al.*

Outline

- **Basics of NV centers in diamond**
  - Structure
  - Optical & magnetic properties

- **Basics of magnetic resonance**

- **Quantum sensing**
  - AC magnetometry
  - Detection of proton spin ensemble
  - Detection and control of a single proton spin

Quantum sensing of nuclear spins

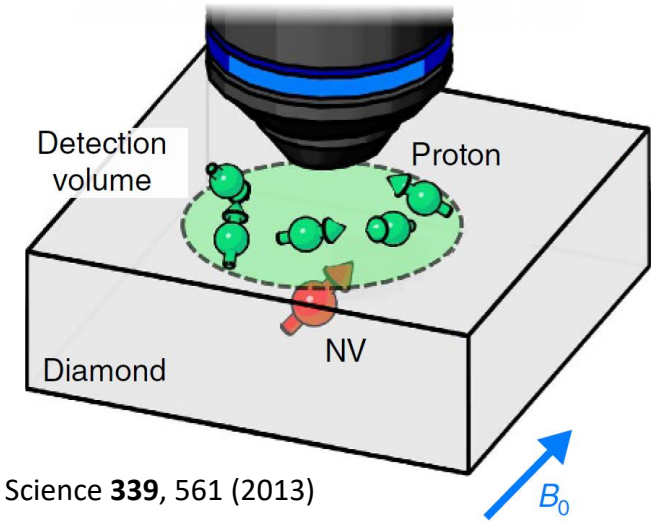

Science **339**, 561 (2013)

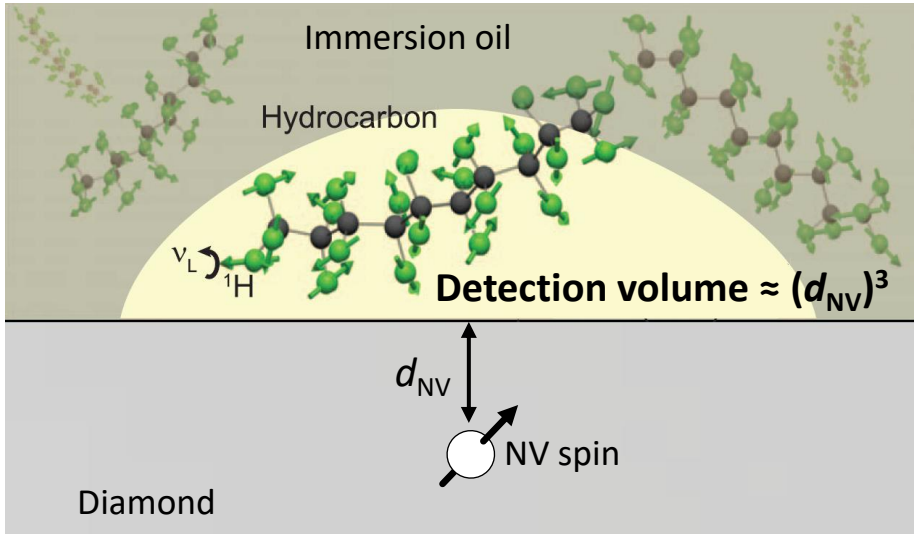

Nature Commun. **6**, 8527 (2015)

Nuclear spins **precess** at f_{ac} = a few kHz–MHz under B_0

⇨ **Weak AC magnetic field** on the NV spin

⇨ Detect using **quantum coherence** of the NV spin

AC magnetometry

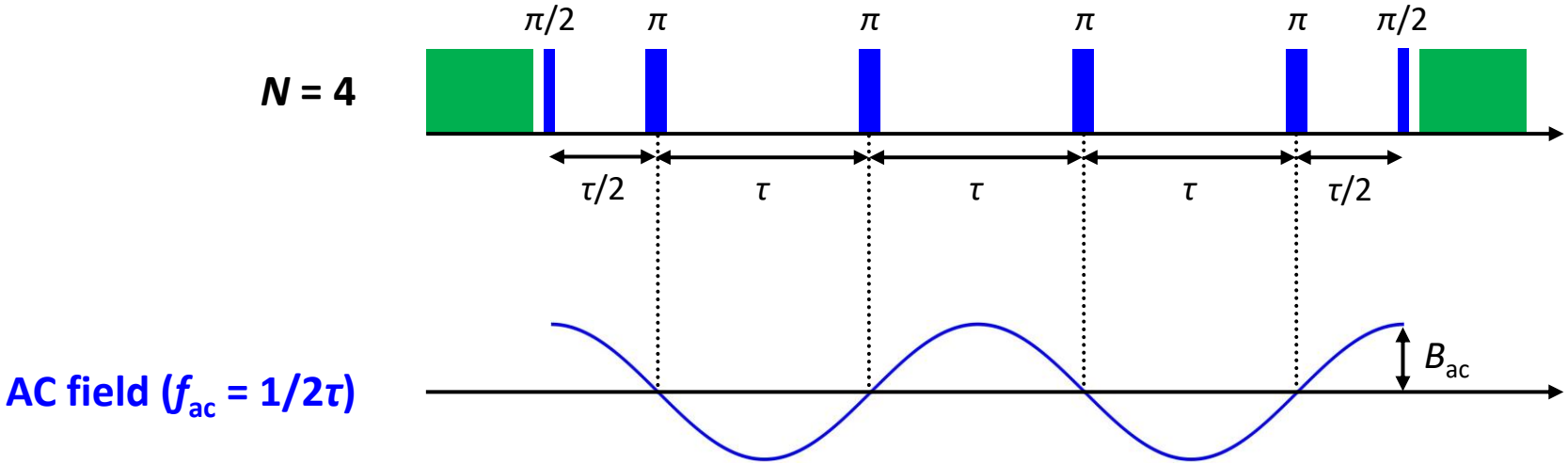

Sensor phase buildup (deviation from *y* axis): *loss of coherence*

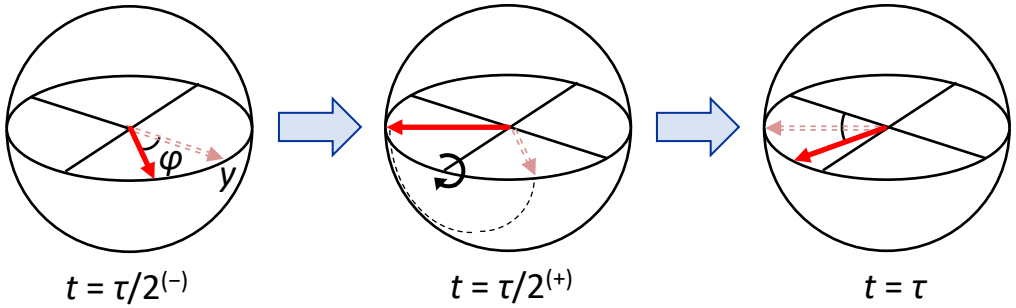

$\varphi(\tau) = 2\varphi(\tau/2)$

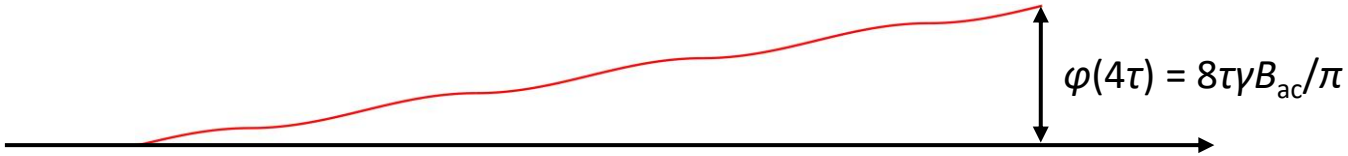

AC magnetometry

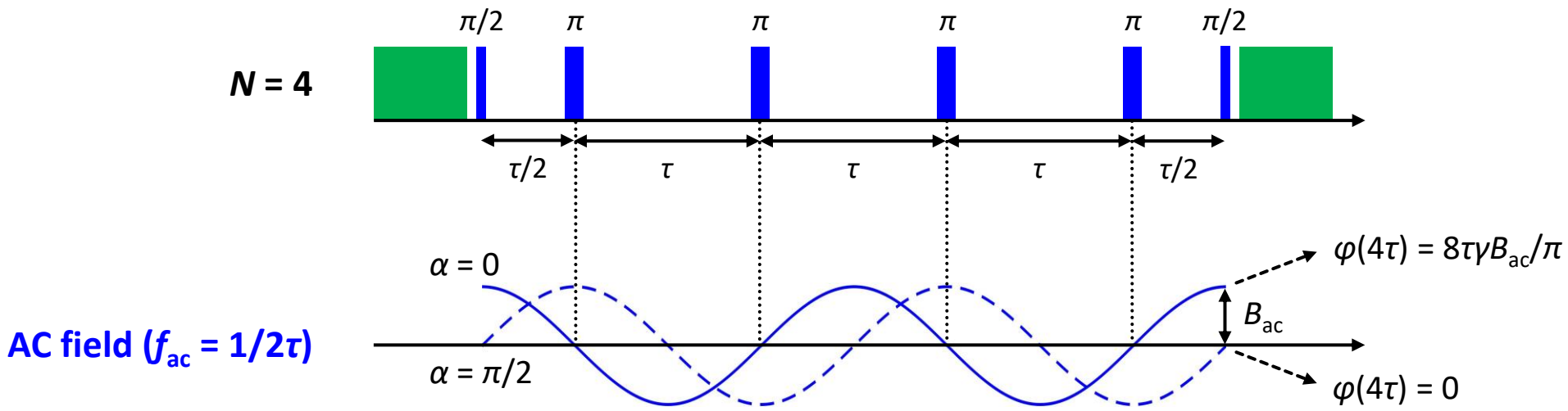

Sensor phase buildup (deviation from *y* axis): *the initial phase α matters*

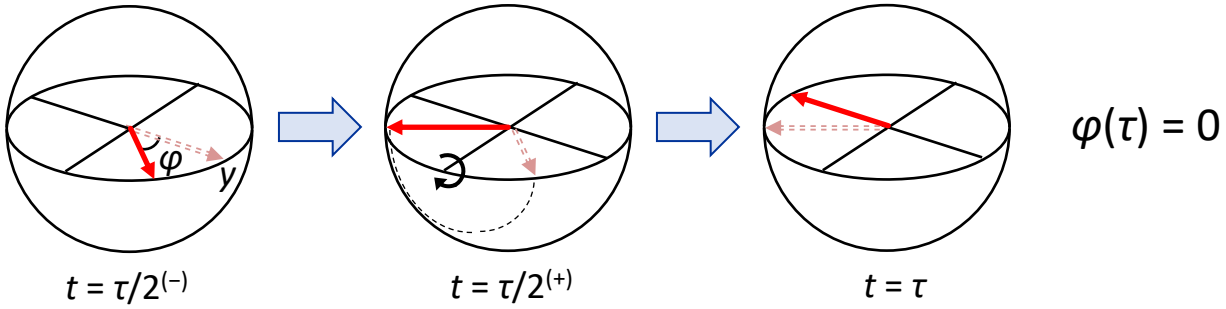

$\varphi(\tau) = 0$

- $\varphi \propto \cos\alpha$
- Usually, we average over **random *α***

Sensing of ensemble nuclear spins

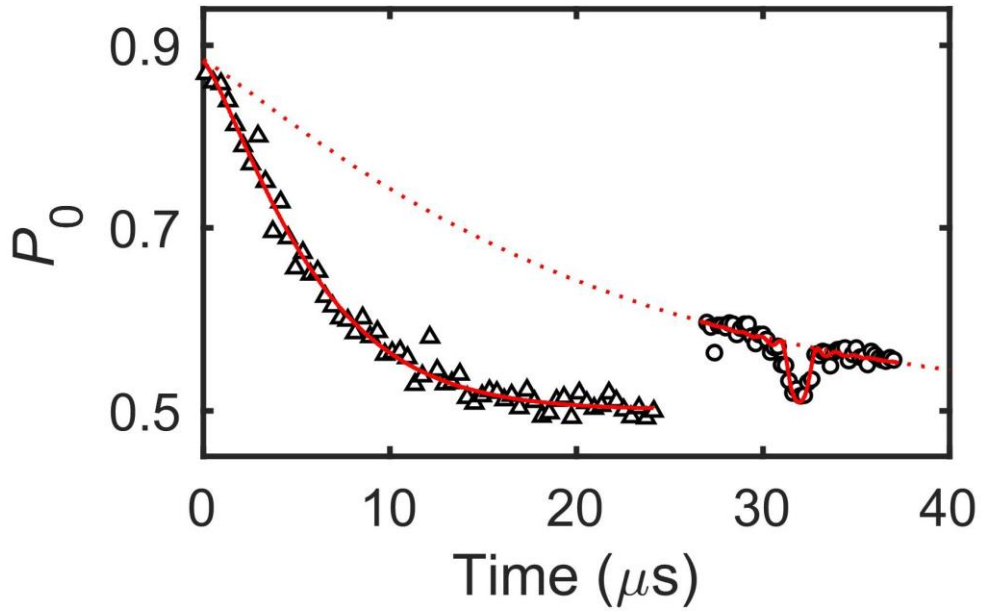

- T_2 = 6.2 µs @B_0 = 23.5 mT
- N = 64
- 2τ = 2 x 32 µs/64 = 1 µs → $\gamma_H B_0$ = (42.577 kHz/mT) x B_0 = 1.00 MHz

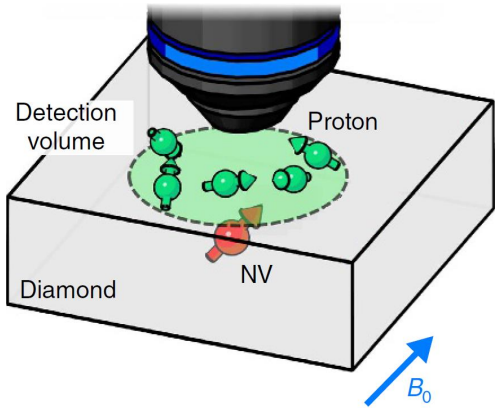

AIP Adv. **10**, 025206 (2020) Misonou *et al.*

Sensing of ensemble nuclear spins

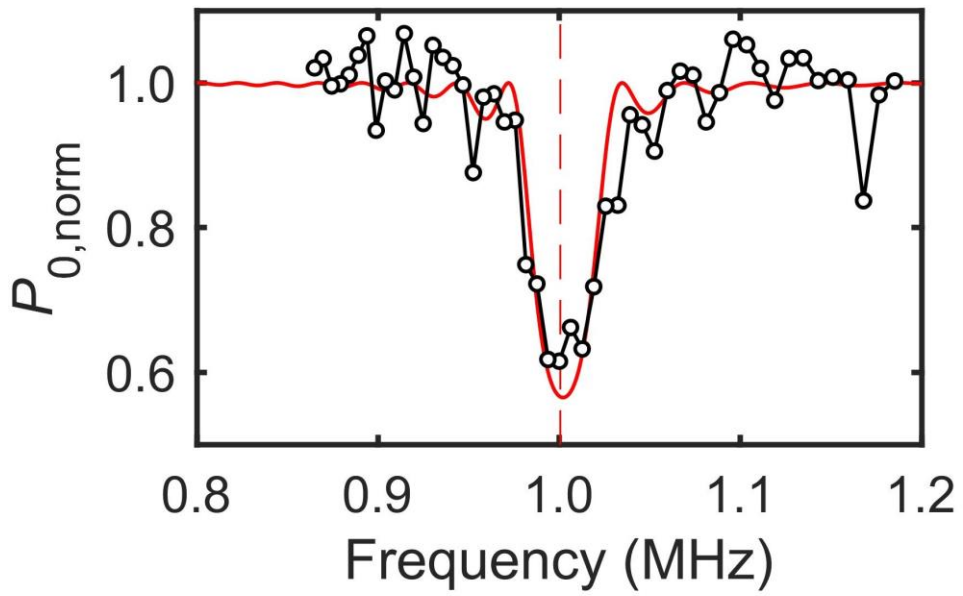

Fit by $C(\tau) = f(B_{\mathrm{rms}})$

$$B_{\mathrm{rms}} = \frac{\mu_0}{4\pi} h\gamma_{\mathrm{H}} \sqrt{\frac{5\pi\rho}{96 d_{\mathrm{NV}}^3}}$$

The explicit form of $C(\tau)$ is given in Phys. Rev. B **93**, 045425 (2016)

- Proton density ρ = 6 x 10^{28} m^{-3} (known)
- d_{NV} = 6.26 nm
- B_{rms} ≈ 560 nT
- Detection volume $(d_{NV})^3$ ≈ **0.25 zL** (zepto = 10^{-21})
- # of protons $\rho(d_{NV})^3$ ≈ 1500
- Thermal polarization (10^{-7}) vs. statistical fluctuation $(1500)^{0.5}$ ≈ **39**

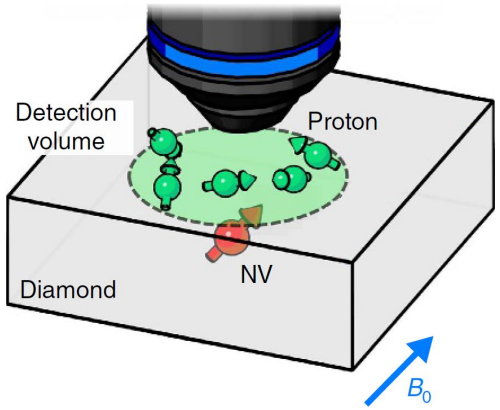

AIP Adv. **10**, 025206 (2020) Misonou *et al.*

Toward single-molecule imaging

- **High spatial resolution**
  - → Special to *single-nuclear-spin-level* NMR
  - → Measure the positions of individual nuclear spins in a single molecule

- **High spectral resolution**
  - → Routine in conventional ensemble NMR spectroscopy
  - → Measure nuclear species (^{1}H, ^{13}C, ^{19}F…)
  - → Measure *J*-couplings & chemical shifts with ppm accuracy

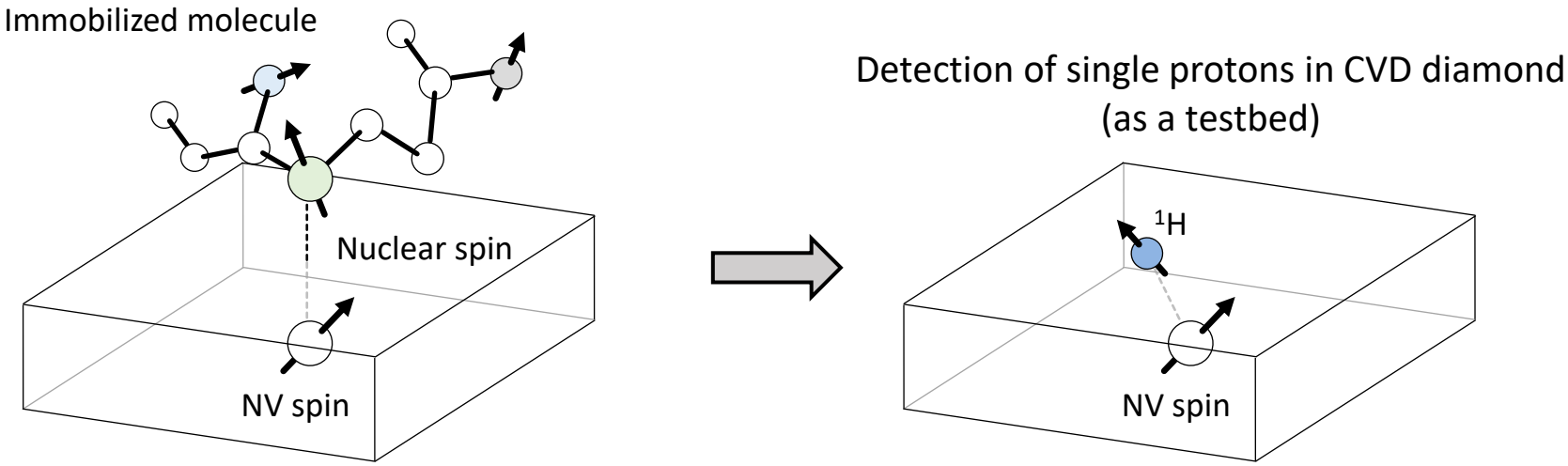

Sensing of single proton spin

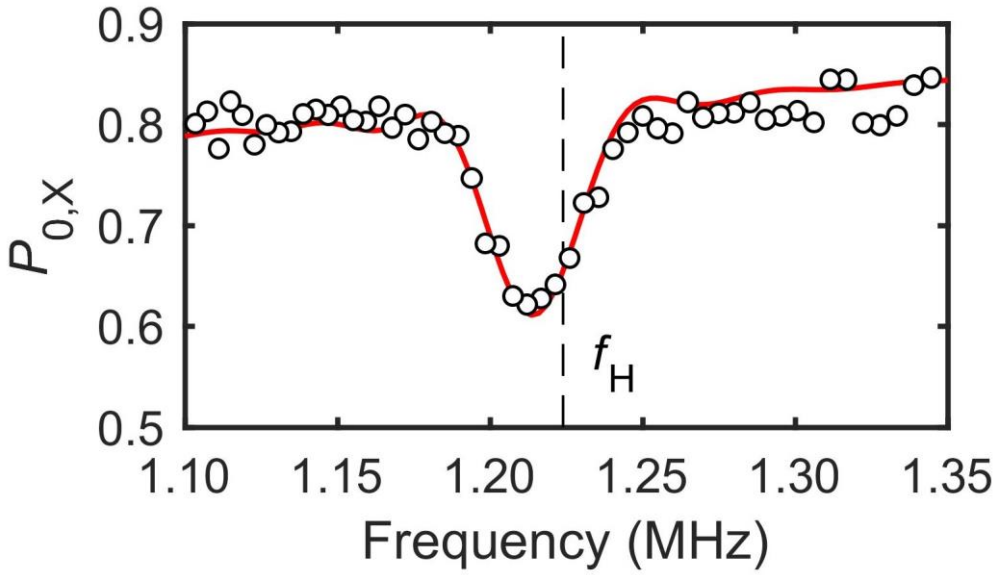

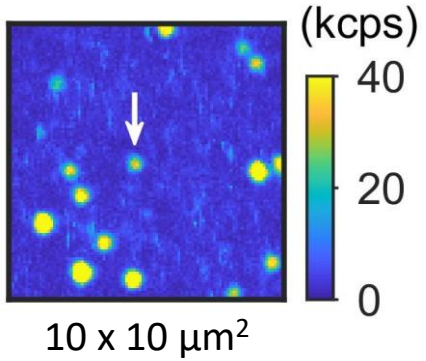

- Single NV in a N-doped CVD film ([^{12}C] = 99.999%)
- N = 64
- $f_H = \gamma_H B_0$ = 42.577 kHz/mT x 28.7 mT = 1.2239 MHz

Appl. Phys. Lett. **117**, 114002 (2020) Sasaki *et al.*

Correlation spectroscopy

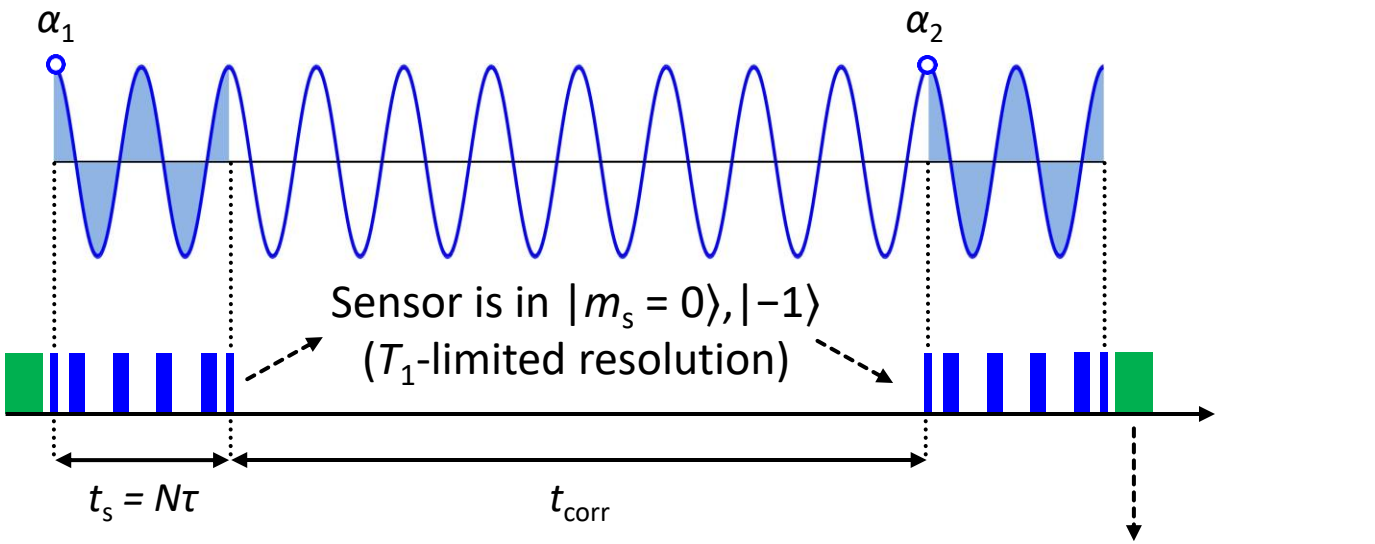

→ Sweep t_{corr}

The transition probability for random phases (α)

$$p(t_1) \approx \frac{1}{2}\left\{1 - \frac{1}{2}\left(\frac{\gamma B_{ac} t_s}{\pi}\right)^2 \cos(2\pi f_{ac} t_{corr})\right\}$$

Nature Commun. **4**, 1651 (2013) Laraoui *et al.*
Phys. Rev. Appl. **4**, 024004 (2015) Kong *et al.*
Nature Commun. **6**, 8527 (2015) Staudacher *et al.*
Phys. Rev. Lett. **116**, 197601 (2016) Boss *et al.*

Correlation spectroscopy of single proton spin

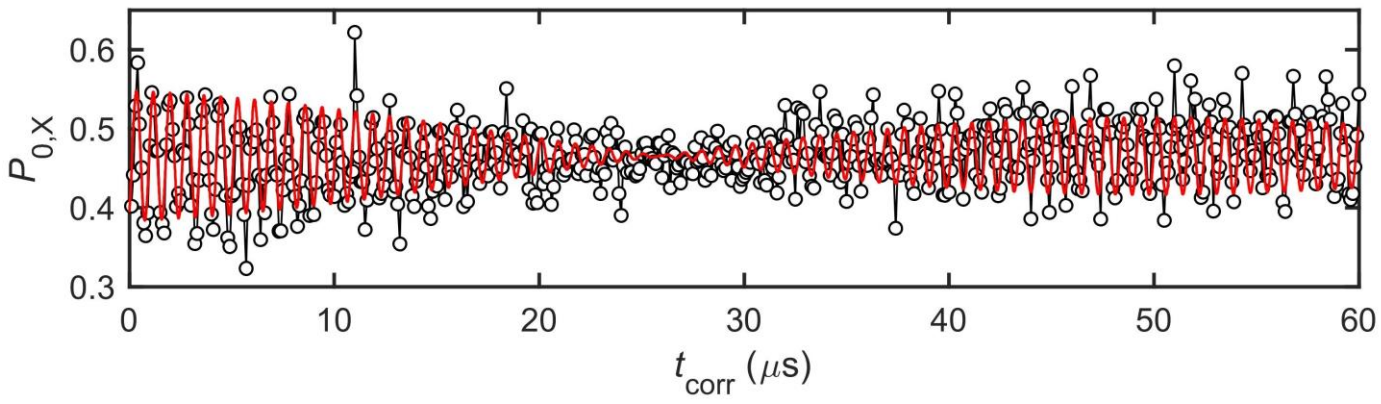

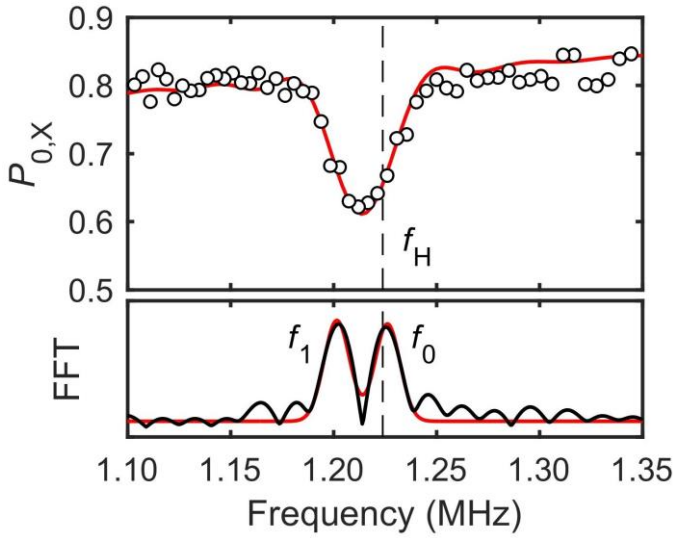

- f_0 = 1.2234 MHz
- f_1 = 1.2046 MHz

Appl. Phys. Lett. **117**, 114002 (2020) Sasaki *et al.*

Correlation spectroscopy of single proton spin

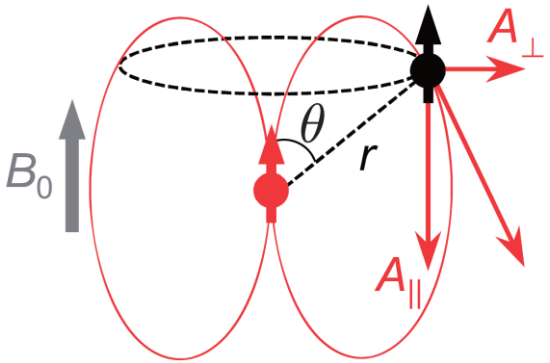

Hamiltonian of ^{1}H nuclear spin coupled with NV spin

$$H_{\mathrm{n}} = f_{\mathrm{H}} I_z + |m_s = -1\rangle\langle -1|(A_\parallel I_z + A_\perp I_x)$$

→ No hyperfine field when $|m_s = 0\rangle$

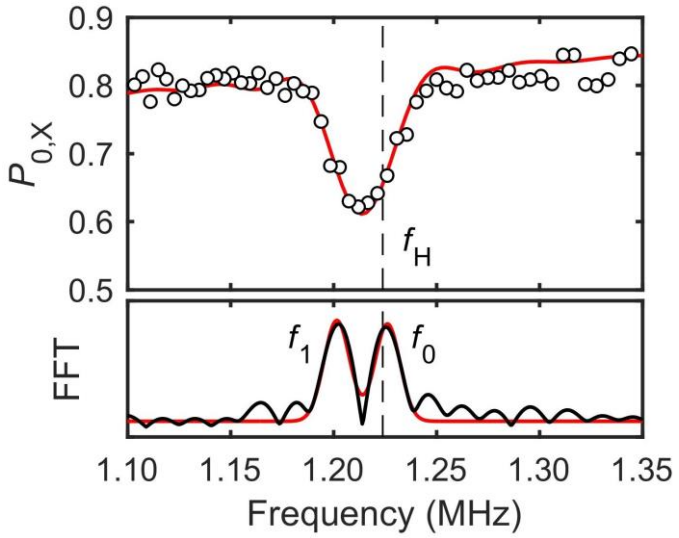

- f_0 = 1.2234 MHz = f_H (m_s = 0)
- f_1 = 1.2046 MHz = $f_H + A'_\parallel$ (m_s = −1)

$A'_\parallel$ = −18.8 kHz
$(f_0 + f_1)/2$ = 1.2140 MHz → dip

Appl. Phys. Lett. **117**, 114002 (2020) Sasaki *et al.*

Coherent control of single proton spin

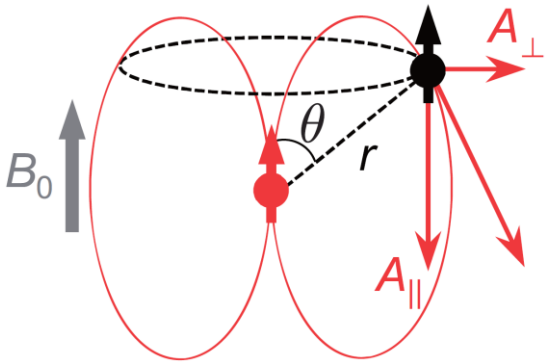

Hamiltonian of ^{1}H nuclear spin coupled with NV spin

$$H_{\mathrm{n}} = f_{\mathrm{H}} I_z + |m_s = -1\rangle\langle -1|(A_\parallel I_z + A_\perp I_x)$$

→ The single proton spin rotates about the $A_\perp$ axis

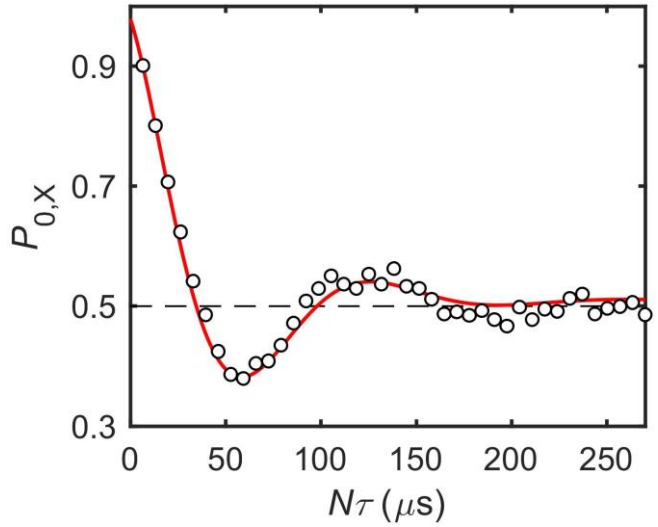

- N up to 656 (τ = 411.5 ns, fixed)
- f_{osc} = 7.414 kHz = $A'_\perp/2$

Appl. Phys. Lett. **117**, 114002 (2020) Sasaki *et al.*

Coherent control of single proton spin

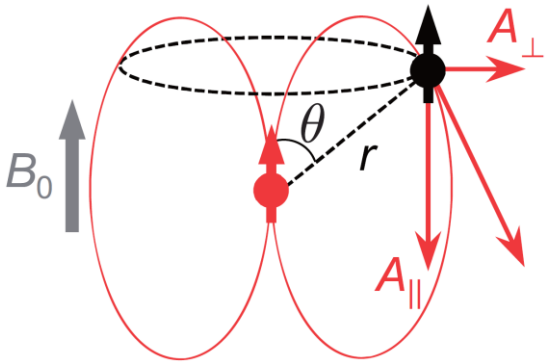

Transition probability of the NV spin

$$P_{0,\mathrm{X}} = 1 - \frac{1}{2}(1 - \underbrace{\boldsymbol{n}_0 \cdot \boldsymbol{n}_{-1}}_{-1}) \sin^2 \frac{N\phi_{\mathrm{cp}}}{2}$$

The explicit forms of $\boldsymbol{n}_0, \boldsymbol{n}_{-1}, \phi_{\mathrm{cp}}$ are given in Phys. Rev. Lett. **109**, 137602 (2012)

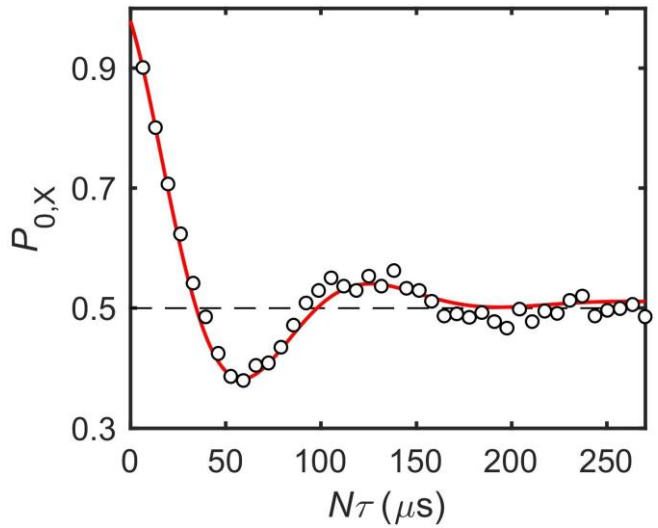

- N up to 656 (τ = 411.5 ns, fixed)
- f_{osc} = 7.414 kHz = $A'_\perp/2$

$P_{0,X} < 0.5$ (coherent rotation)
→ Single proton

Appl. Phys. Lett. **117**, 114002 (2020) Sasaki *et al.*

Conditional rotation of single nuclear spin

Electron spin control

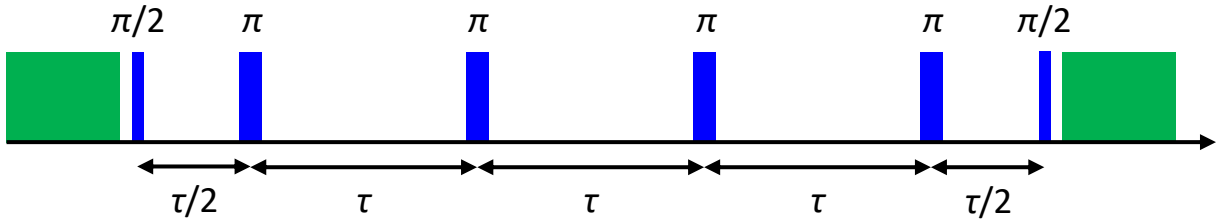

Evolution of nuclear spin vector

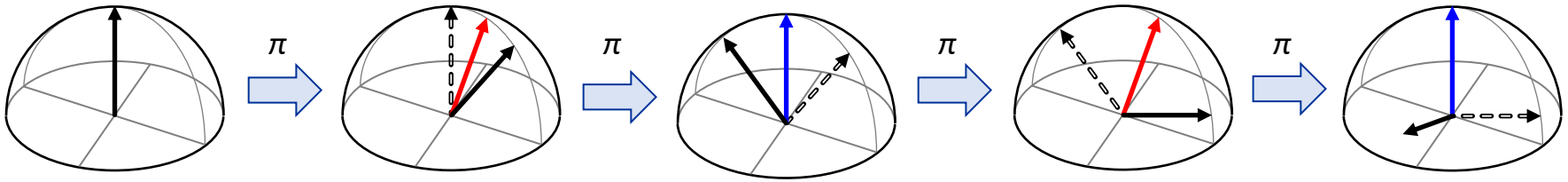

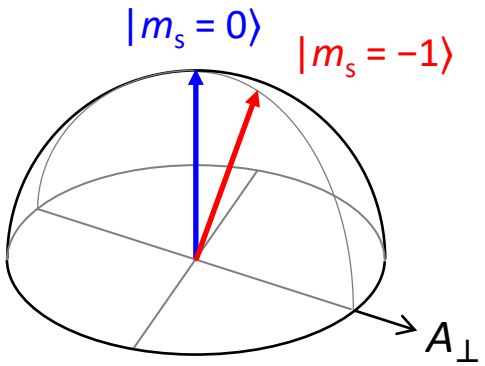

q-axis of nuclear spin

***Start from* $|m_s = 0\rangle$**

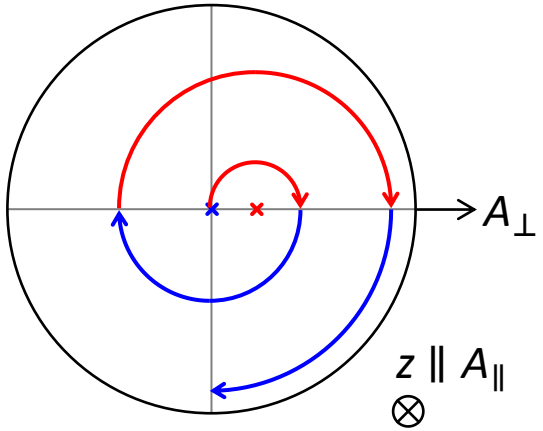

***Start from* $|m_s = -1\rangle$**

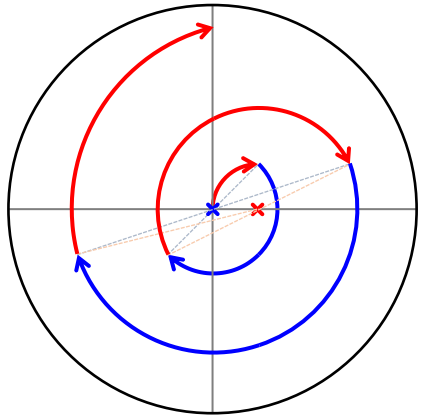

Determination of hyperfine constants

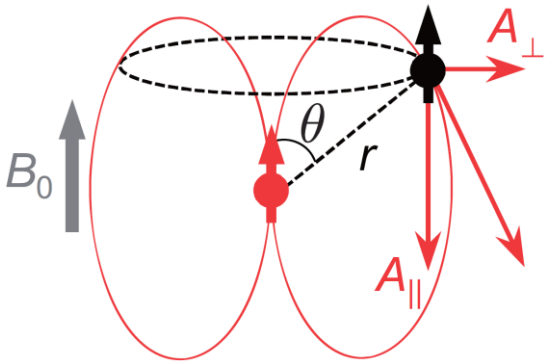

Magnetic dipole interaction

$$A_\parallel = h\gamma_e\gamma_H \frac{3\cos^2\theta - 1}{r^3}$$

$$A_\perp = h\gamma_e\gamma_H \frac{3\cos\theta\sin\theta}{r^3}$$

$A_\parallel$ = −19.0 kHz
$A_\perp$ = 22.9 kHz

⟺

r = 1.44 nm
θ = 72.3°

The position of the nucleus can be determined
→ Basis for single-molecule structure analysis

(Azimuthal angle ϕ can determined by RF control) Phys. Rev. B **98**, 121405 (2018) Sasaki *et al.*

Appl. Phys. Lett. **117**, 114002 (2020) Sasaki *et al.*

Magnetic field dependence

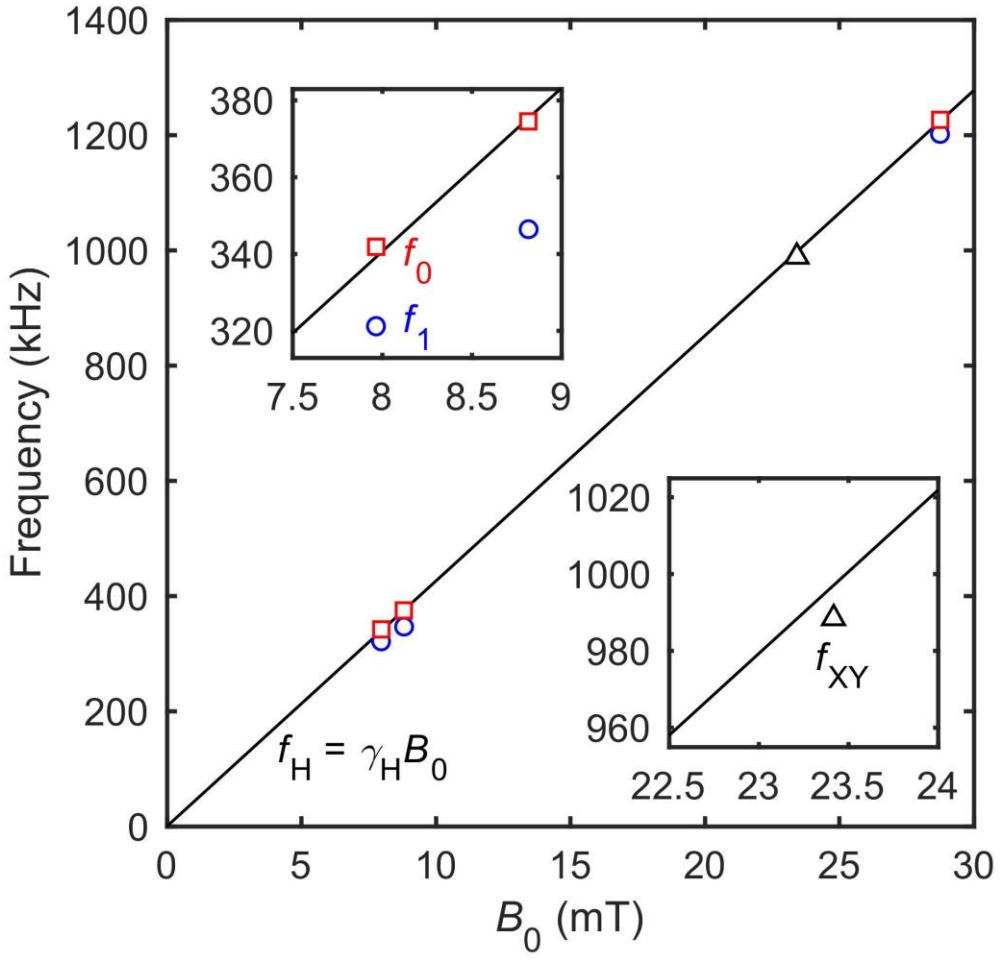

(γ_H/γ_C = 3.97 → Spurious harmonics?) Phys. Rev. X **5**, 021009 (2015) Loretz *et al.*

Appl. Phys. Lett. **117**, 114002 (2020) Sasaki *et al.*

Toward single-molecule imaging

- **High spatial resolution**
  - → Accurate measurement of electron–nuclear interaction parameters ($A_{\parallel}$, $A_{\perp}$) ≈ (r, θ)
  - → ϕ can also be determined by RF control of nuclear spin

- **High spectral resolution**
  - → Routine in conventional ensemble NMR spectroscopy
  - → Measure nuclear species (^{1}H, ^{13}C, ^{19}F…)
  - → Measure *J*-couplings & chemical shifts with ppm accuracy

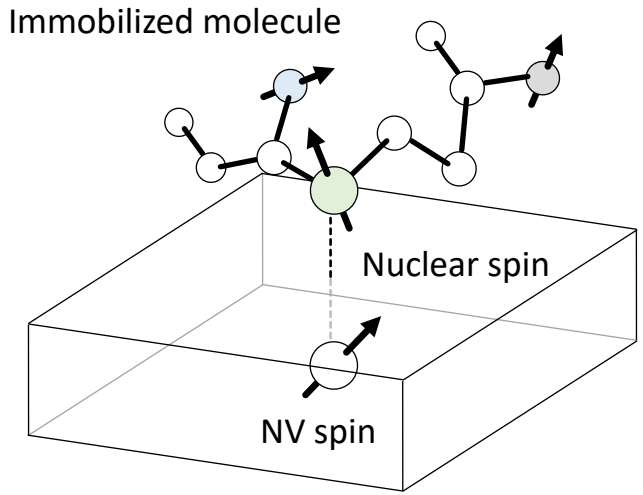

Not so easy with NV centers

Resolution limited by sensor/memory spin lifetimes ($T_{2e/n}$, $T_{1e/n}$)

T_{2e} tends to be shorter for near-surface NV centers

AC magnetometry revisited

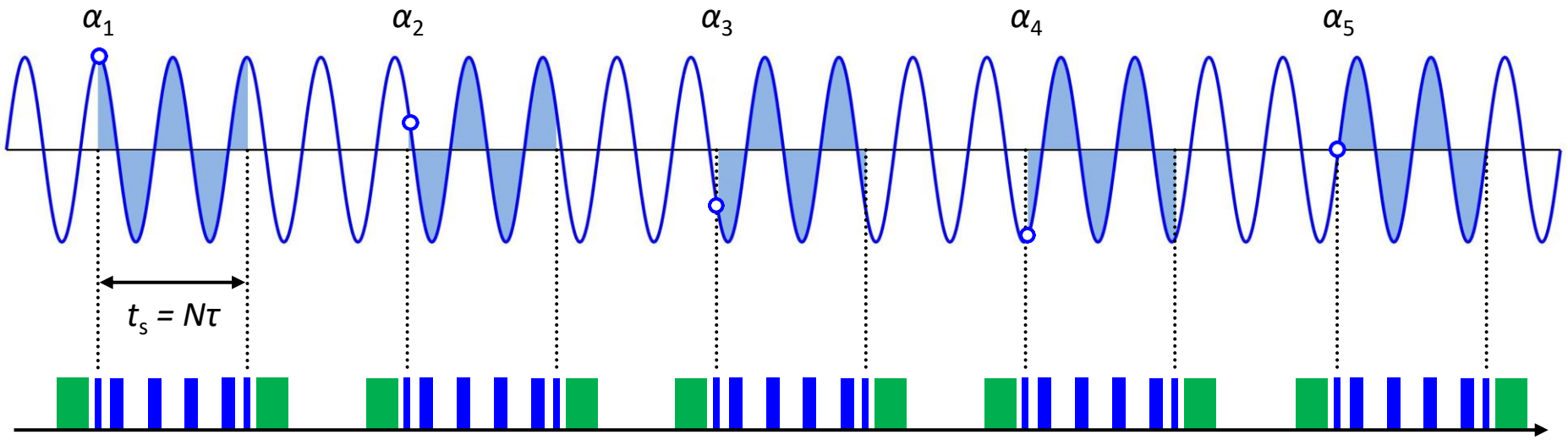

- $\varphi \propto \cos \alpha$
- Usually, we average over **random α**

AC magnetometry revisited

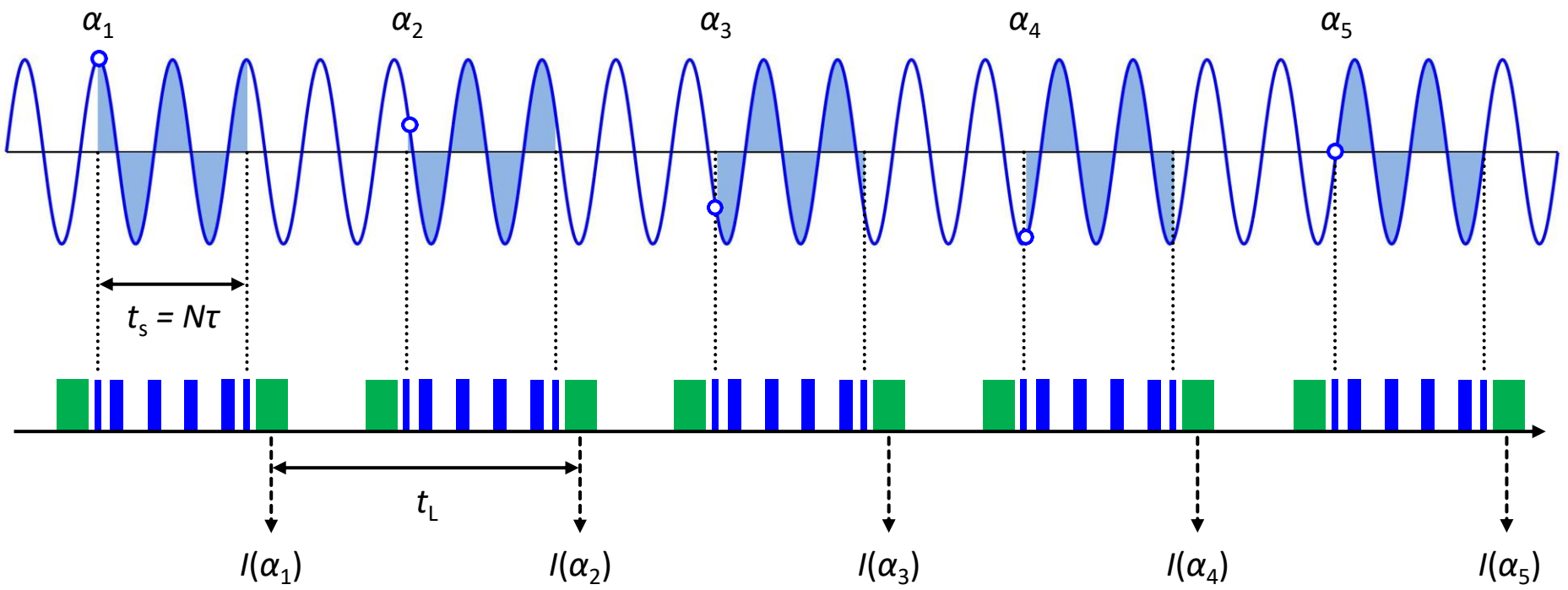

- $\varphi \propto \cos \alpha$
- Usually, we average over **random α**
- **If the data acquisition is periodic,** adjacent α's are related by $\alpha_{k+1} = 2\pi f_{ac} t_L + \alpha_k$

Ultrahigh resolution sensing

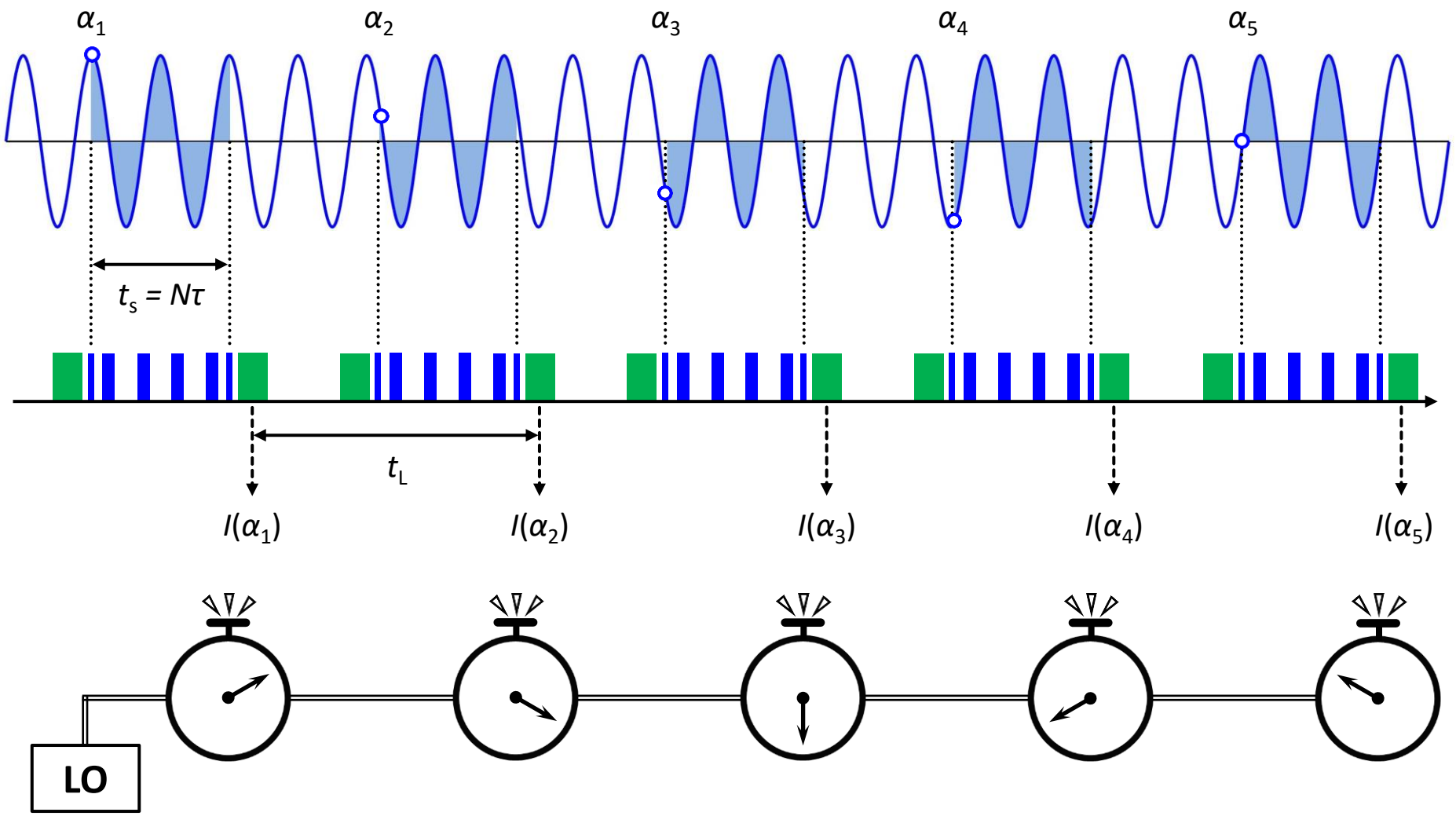

Undersampled, sensor-lifetime-unlimited signal

Science **356**, 832 (2017) Schmitt *et al.*
Science **356**, 837 (2017) Boss *et al.*
Nature **555**, 351 (2018) Glenn *et al.*

Ultrahigh resolution sensing

B_{ac} = 96.5 nT & f_{ac} = 2.001 MHz applied from a coil, detected by a single NV center

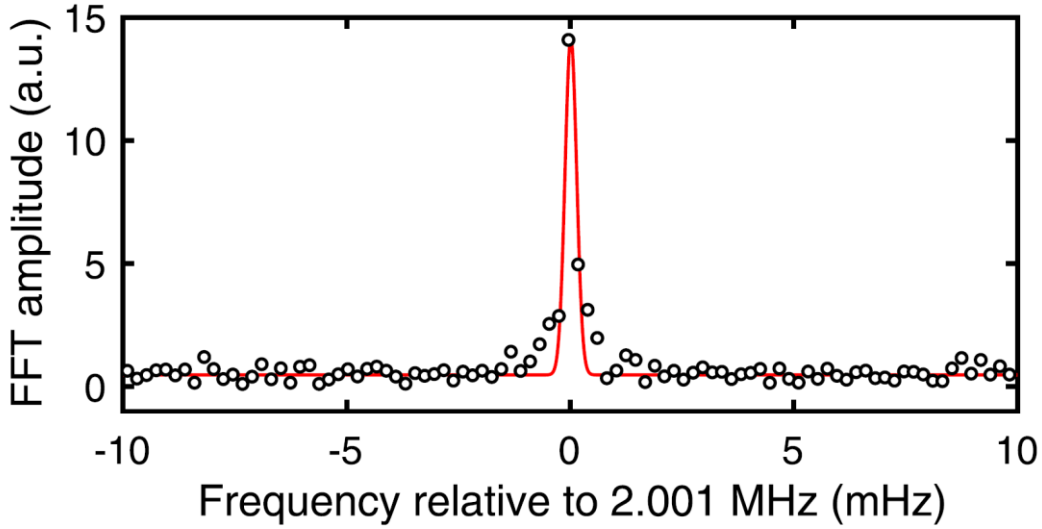

- T = 3600 sec
- FWHM = 0.304 mHz

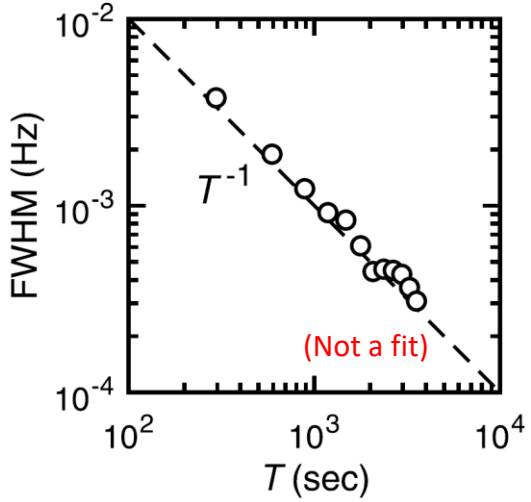

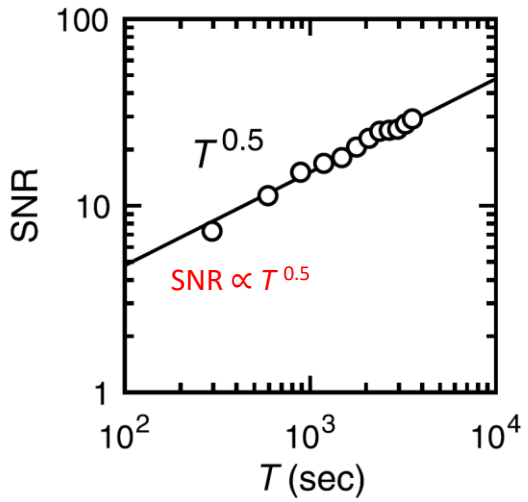

J. Appl. Phys. **123**, 161101 (2018) Abe *et al.*

Free induction decay of single proton spin

RF control & free precession of proton spin

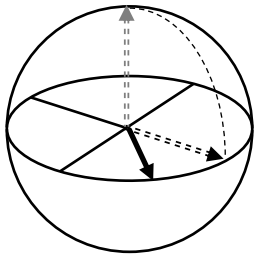

Nuclear Rabi oscillation

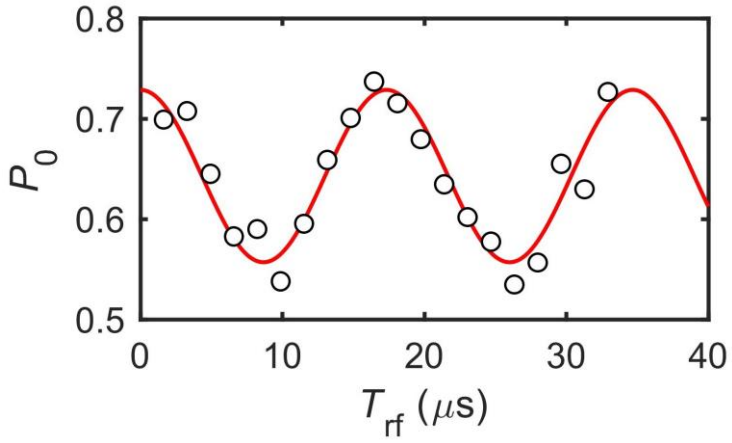

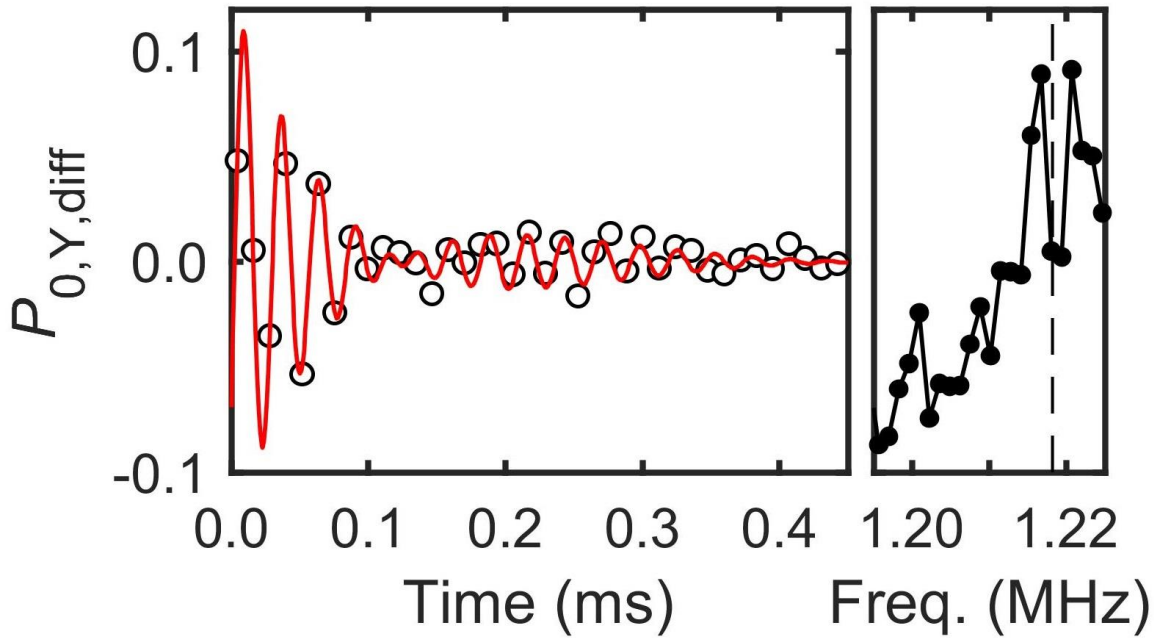

- $T_{rf,\,\pi/2}$ = 4.115 μs
- [PulsePol]–$T_{rf,\,\pi/2}$–[X/2–(XY16)–Y/2–L_{RO}]^{50}
- $f_{sample} = 1/t_L$ = 84.46 kHz
- $f_p = (f_0+f_1)(t_s/t_L)/2+f_0(t_s-t_L)/t_L$ = 1.2182 MHz
  → Split (analogous to chemical shifts)

Appl. Phys. Lett. **117**, 114002 (2020) Sasaki *et al.*

Summary

- **Tools for single-molecule imaging/structure analysis are being developed**[1],
  - → Ultrahigh resolution sensing[2,3,4], resolving chemical shifts[4,5] & suppression of back action from nuclear spins[6,7]
  - → Determination of the positions of individual nuclear spins via RF control[8,9,10,11]
  - → Detection & control of single proton spins[12,13]
- **^{13}C nuclear spin cluster as a quantum simulator/computer**[14,15]

[1] Rev. Mod. Phys. **96**, 025001 (2024) Du *et al.*
[2] Science **356**, 832 (2017) Schmitt *et al.* (Ulm)
[3] Science **356**, 837 (2017) Boss *et al.* (ETH)
[4] Nature **555**, 351 (2018) Glenn *et al.* (Harvard)
[5] Science **357**, 67 (2017) Aslam *et al.* (Stuttgart)
[6] Nature Commun. **10**, 594 (2019) Pfender *et al.* (Stuttgart)
[7] Nature **571**, 230 (2019) Cujia *et al.* (ETH)
[8] Phys. Rev. B **98**, 121405 (2018) Sasaki *et al.* (Keio)
[9] Phys. Rev. Lett. **121**, 170801 (2018) Zopes *et al.* (ETH)
[10] Nature **576**, 411 (2019) Abobeih *et al.* (Delft)
[11] Nature Commun. **13**, 1260 (2022) Cujia *et al.* (ETH)
[12] Phys. Rev. Lett. **113**, 197601 (2014) Sushkov *et al.* (Harvard)
[13] Appl. Phys. Lett. **117**, 114002 (2020) Sasaki *et al.* (Keio)
[14] Science **374**, 1474 (2021) Randall *et al.* (Delft)
[15] Nature **606**, 884 (2022) Abobeih *et al.* (Delft)